

Supporting Information

A translation of the structure of mussel byssus threads into synthetic materials by the utilization of histidine-rich block copolymers

*Marcel Enke, Ranjita K. Bose, Stefan Zechel, Jürgen Vitz, Robert Deubler, Santiago J. Garcia, Sybrand van der Zwaag, Felix H. Schacher, Martin D. Hager, * Ulrich S. Schubert**

^a Laboratory of Organic and Macromolecular Chemistry (IOMC)

Friedrich Schiller University Jena, Humboldtstr. 10, 07743 Jena (Germany)

^b Jena Center for Soft Matter (JCSM)

Friedrich Schiller University Jena, Philosophenweg 7, 07743 Jena (Germany)

^c Novel Aerospace Materials group

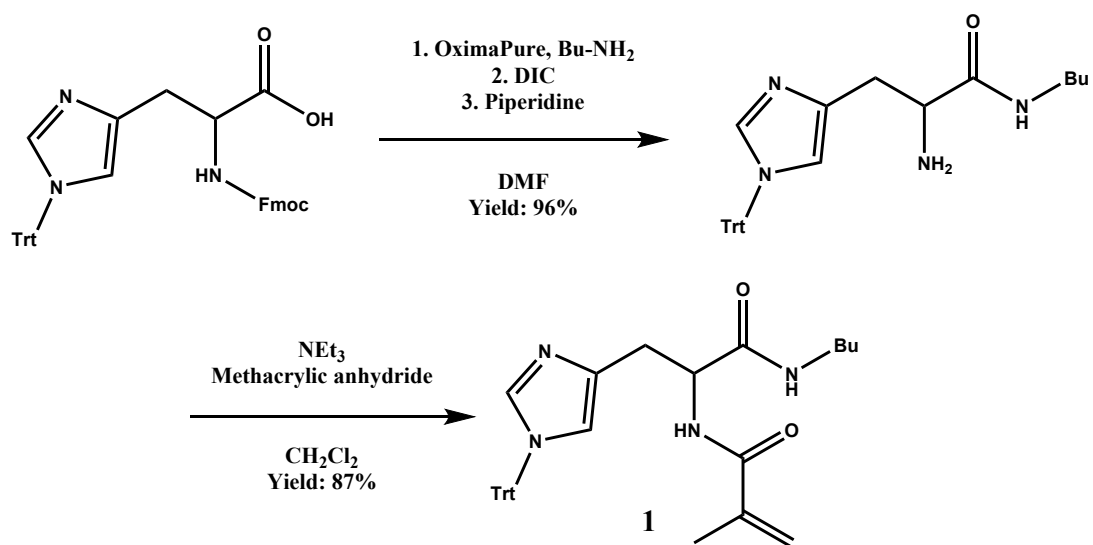
Delft University of Technology, Kluyverweg 1, 2629 HS Delft (Netherlands)

†Current address: Ranjita K. Bose, Engineering and Technology Institute Groningen (ENTEG), University of Groningen, Nijenborgh 4, 9747AG Groningen (Netherlands)

Table of content:

Schemes	S3
Figures	S4
NMR	S4
Kinetic study	S5
SEC	S6
DSC/TGA of polymers	S8
SAXS data of polymers	S17
DSC/TGA of metallopolymers	S18
SAXS data of metallopolymers	S26
Self-healing tests	S27
Nanoindentation	S30
Tables	S31
Experimental section	S34
Density measurements	S38
References	S39

Schemes:



Scheme S1: Schematic representation of the synthesis of the histidine monomer (**1**).

Figures:

NMR:

Figure S1 shows an overlay of the proton NMR spectra of **P1** and **P5**, respectively. The polymer backbone is located between 0.7 to 2.5 ppm and the $-\text{OCH}_2$ groups of PBA between 3.8 to 4.2 ppm. The protons of the histidine are visible at approximately 2.7 to 3.3 ppm and 4.4 to 4.6 ppm. In between 6.3 and 7.5 ppm, the histidine protons overlap with the aromatic protons of styrene. The composition of all compounds was calculated utilizing the signals at 2.7 to 3.3 ppm for 1, 6.3 to 6.9 ppm for PS and 3.8 to 4.2 ppm for PBA.

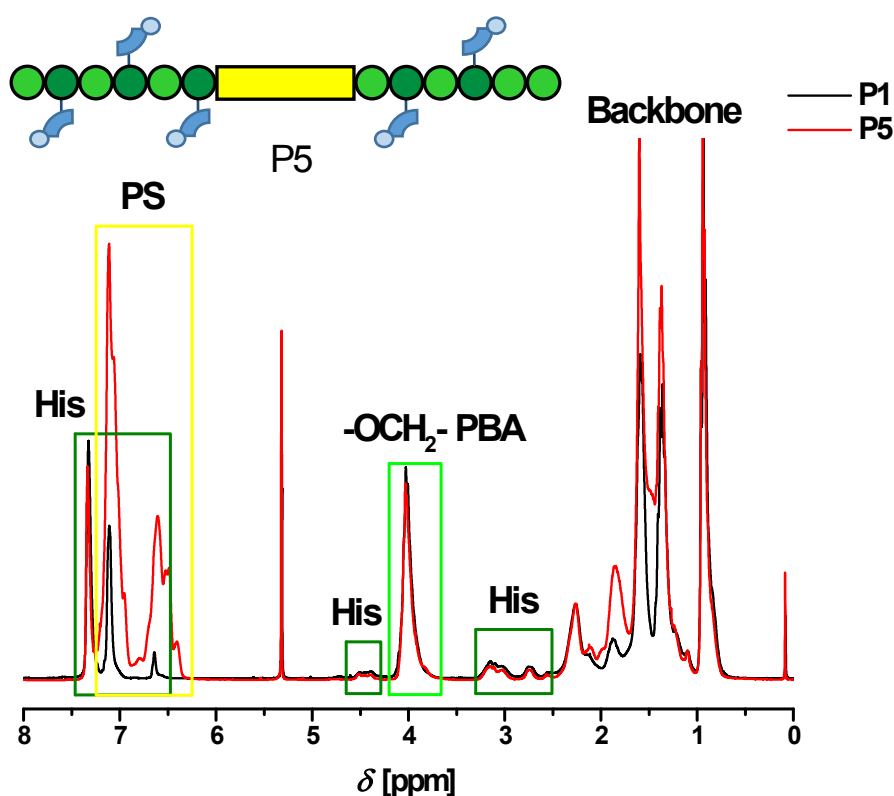
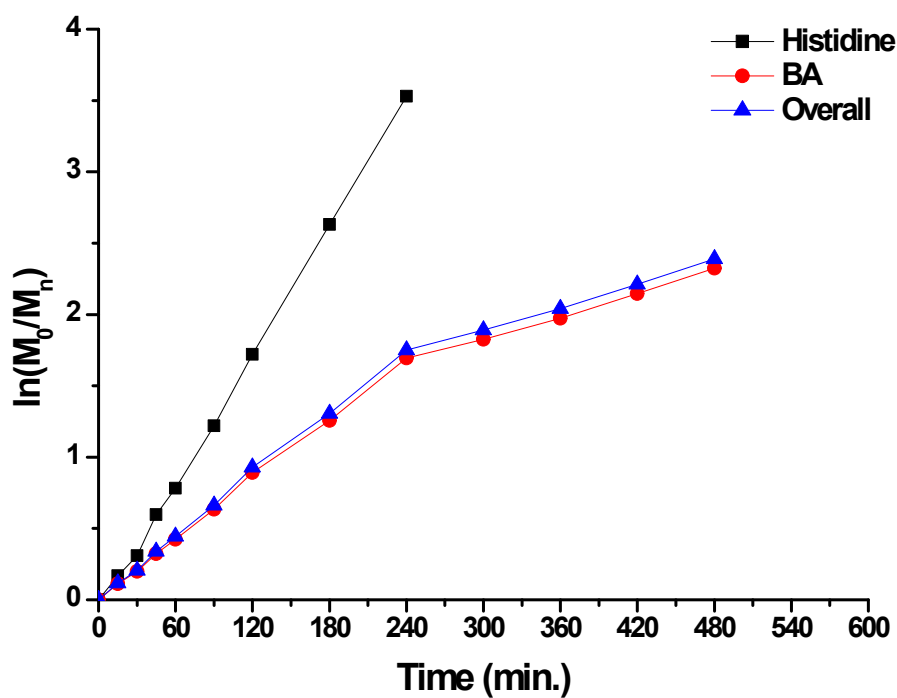


Figure S1: ^1H NMR spectra of **P1** and **P5** (300 MHz, CD_2Cl_2).

Kinetic study:

a)



b)

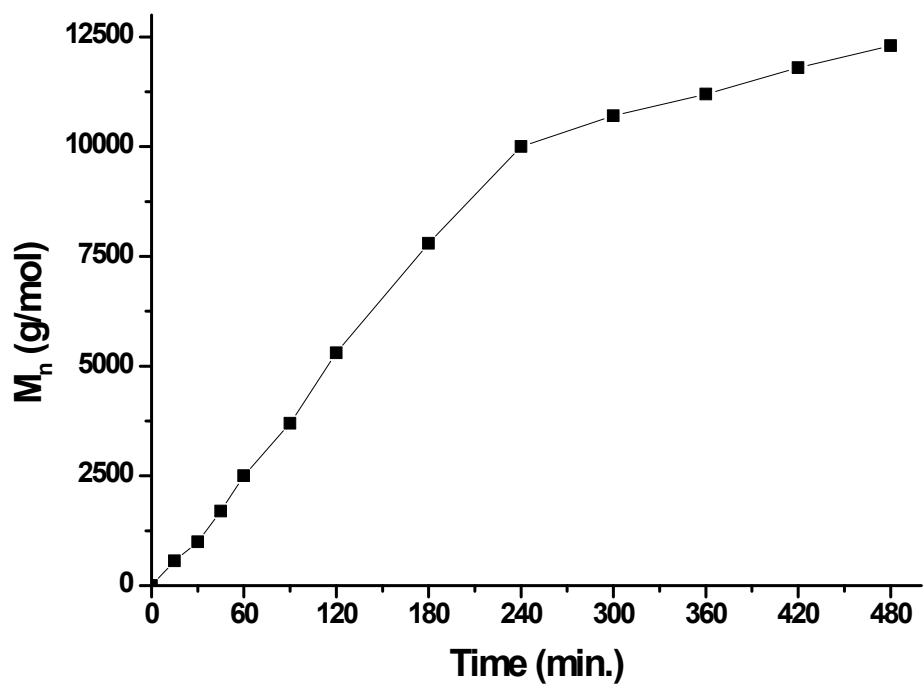


Figure S2: Kinetic study of the conversion of the histidine monomer (1) during the copolymerization with *n*-butyl acrylate (BA) via a) ¹H NMR-spectroscopy and b) size exclusion chromatography (SEC).

SEC:

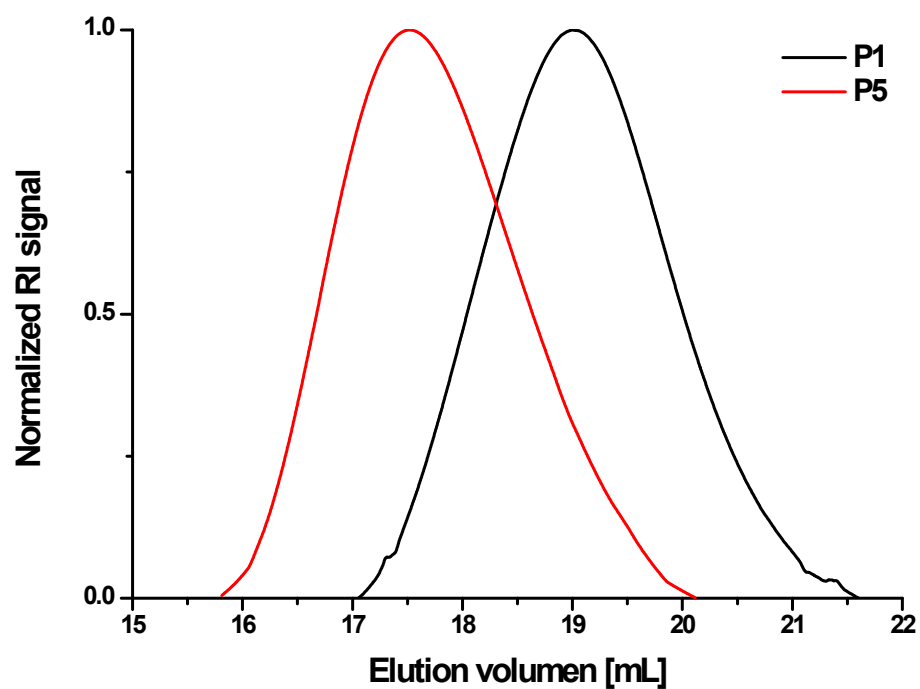


Figure S3: Size exclusion chromatography (SEC) of P1 and P5 (DMAc + 0.21% LiCl).

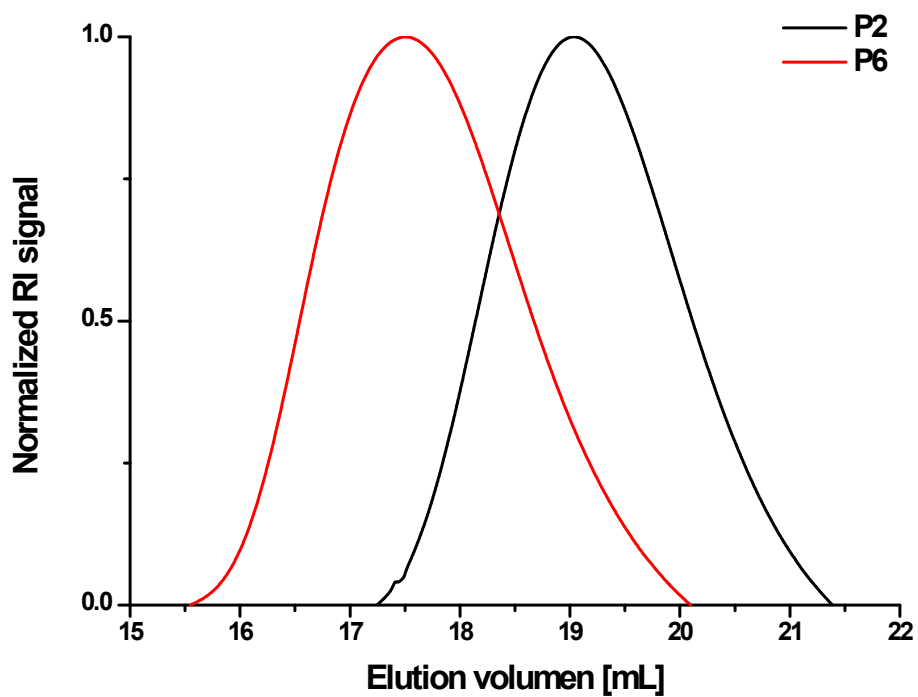


Figure S4: Size exclusion chromatography (SEC) of P2 and P6 (DMAc + 0.21% LiCl).

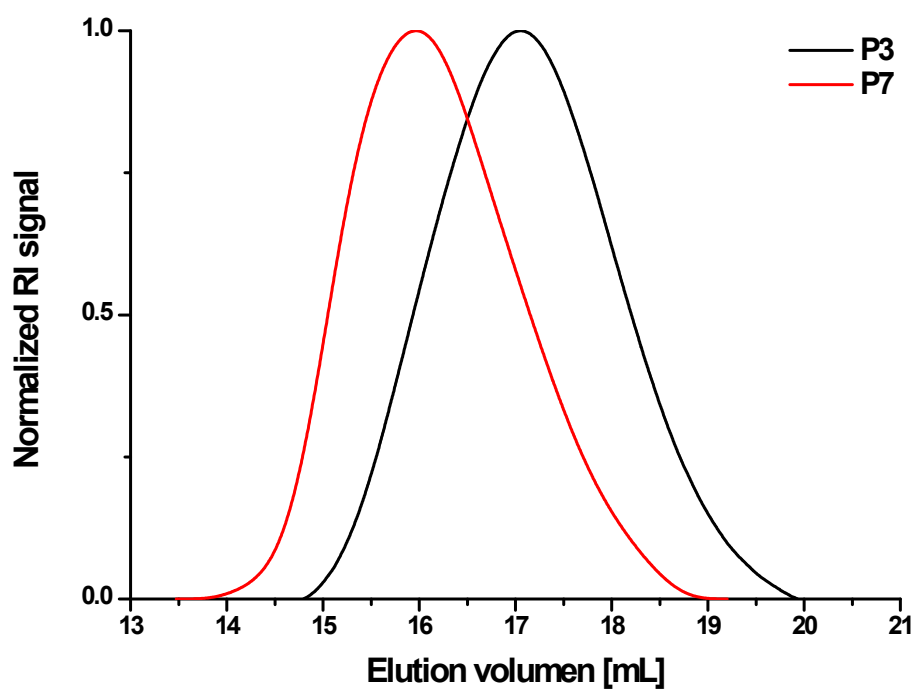


Figure S5: Size exclusion chromatography (SEC) of **P3** and **P7** (DMAc + 0.21% LiCl).

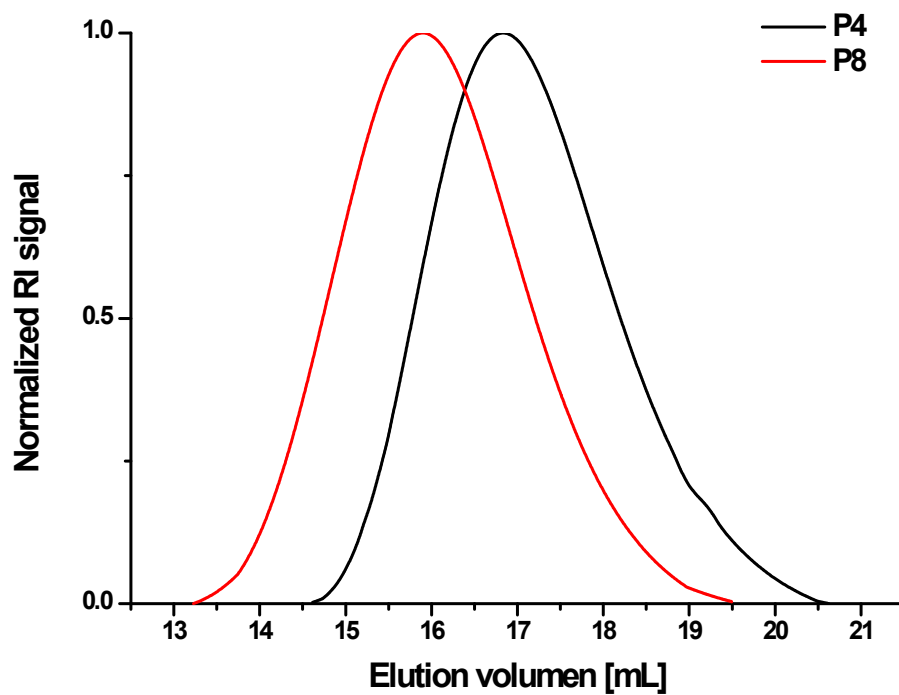
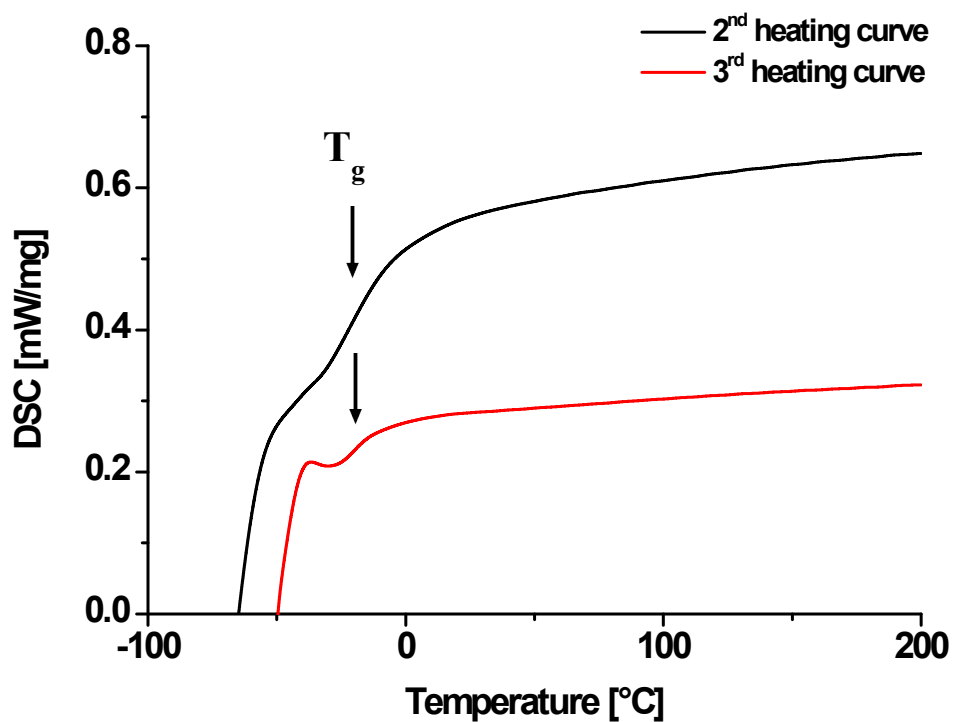


Figure S6: Size exclusion chromatography (SEC) of **P4** and **P8** (DMAc + 0.21% LiCl).

DSC/TGA of polymers:

The T_g of **P1**, which represents the soft block with ligand moieties, is significantly higher compared to the T_g of pure BA (-57.7 °C) due to the presence of the histidine units (Figure S7).[S1] The introduction of polystyrene as hard block causes an increase of the T_g (**P5**, Figure S11). Comparing the measured glass transition temperatures of **P5** and **P6**, revealed that the block structure (A-B-A or B-A-B) have a small influence, so **P5** shows a slightly higher T_g compared to **P6** (Figure S12). Increasing the molar mass of each block segment resulted also in an increase of the glass transition temperatures of the polymers **P3** and **P4** as well as **P7** and **P8**. [S2-S3] Due to the higher molar mass, the block copolymers **P7** and **P8** have two glass transition temperatures, which is presumably caused by phase separation (Figures S13a and S14a).[S4] In general, the A-B-A block copolymers (**P5** and **P7**) have a higher T_g compared to the B-A-B counterparts (**P6** and **P8**). One possible explanation for this behavior might be that the location of the histidine moieties. The ligand copolymerizes faster than BA, which leads to a high concentration of histidine units at the ends of the soft block. As a result, the A-B-A block copolymers have a terminal histidine rich domain, whereas B-A-B block copolymers feature the histidines at the interface to the hard block leading to a lower impact of those groups and, consequently, in a lower glass transition temperature. Thus, these structural variances can lead to these different values of the T_g .

a)



b)

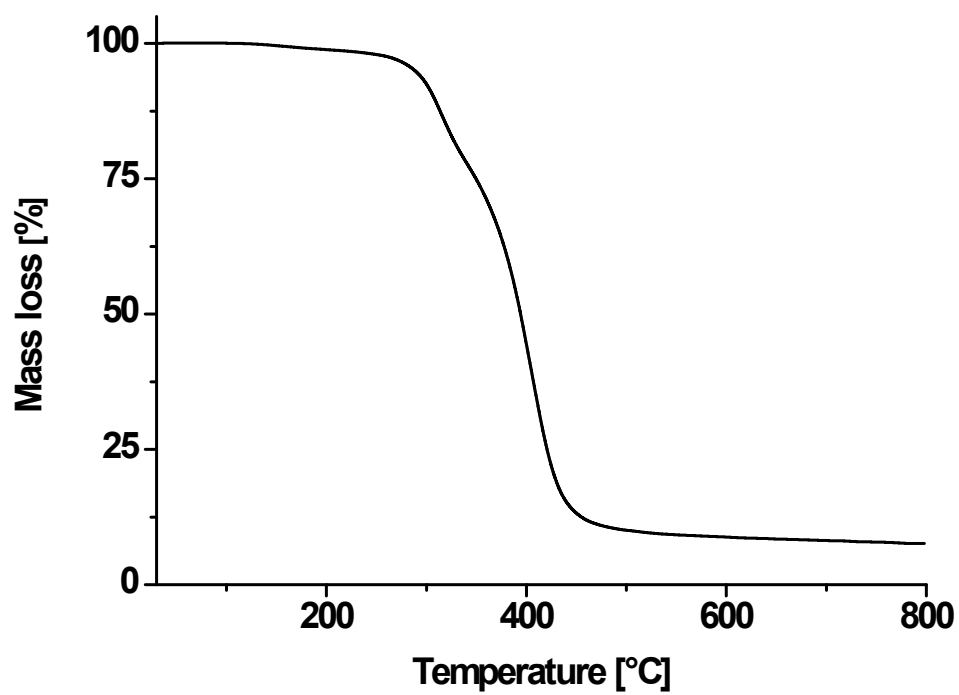
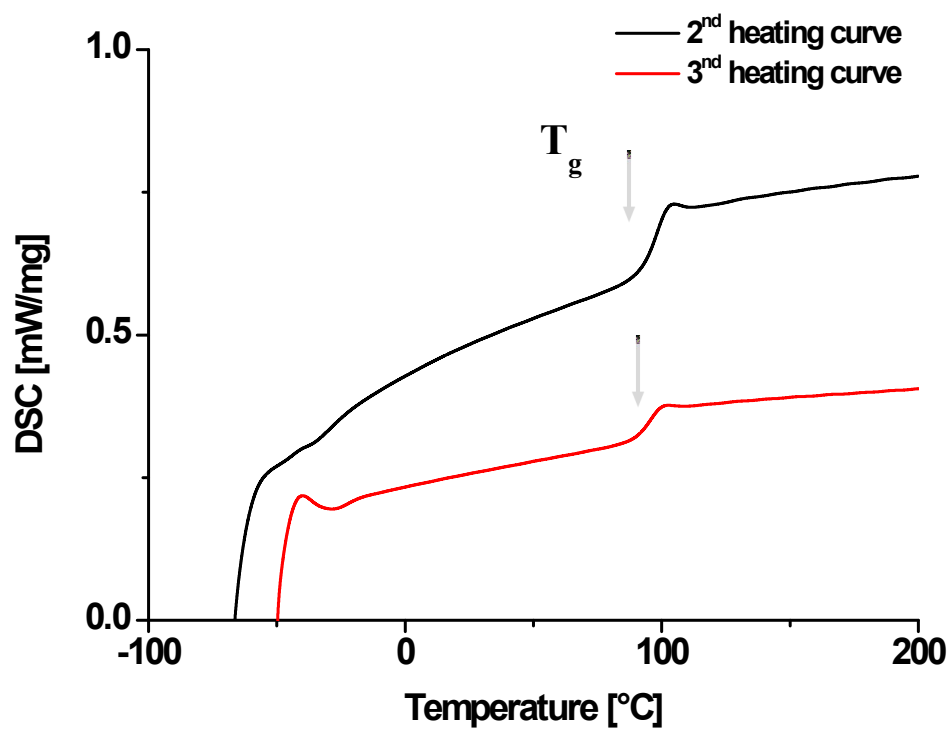


Figure S7: Thermal properties of **P1**. a) DSC curve (2nd heating with 20 K/min and 3rd heating with 10 K/min) and b) TGA curve.

a)



b)

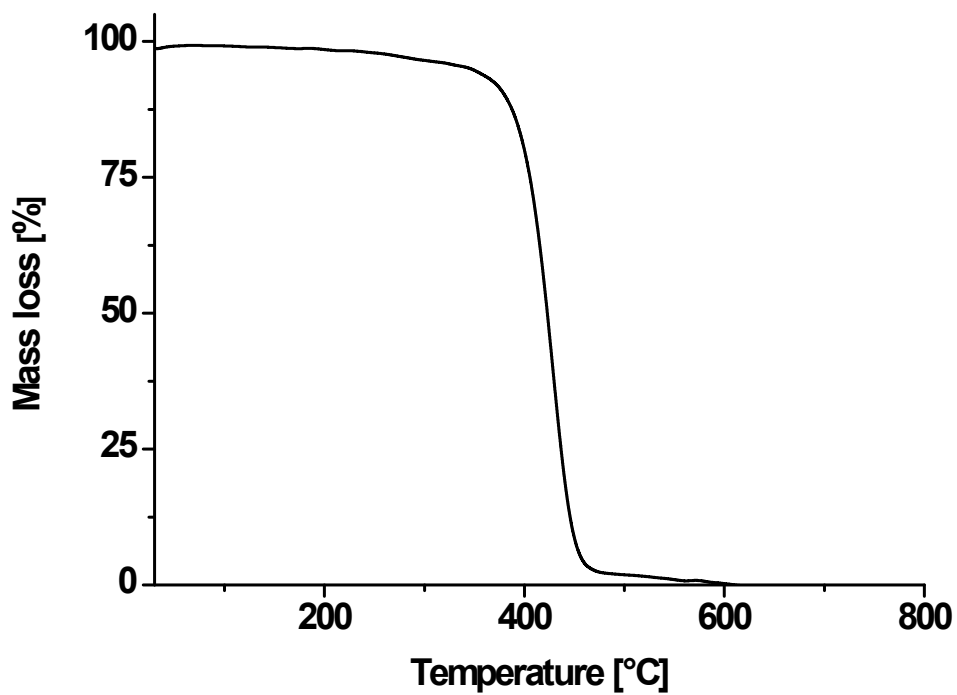
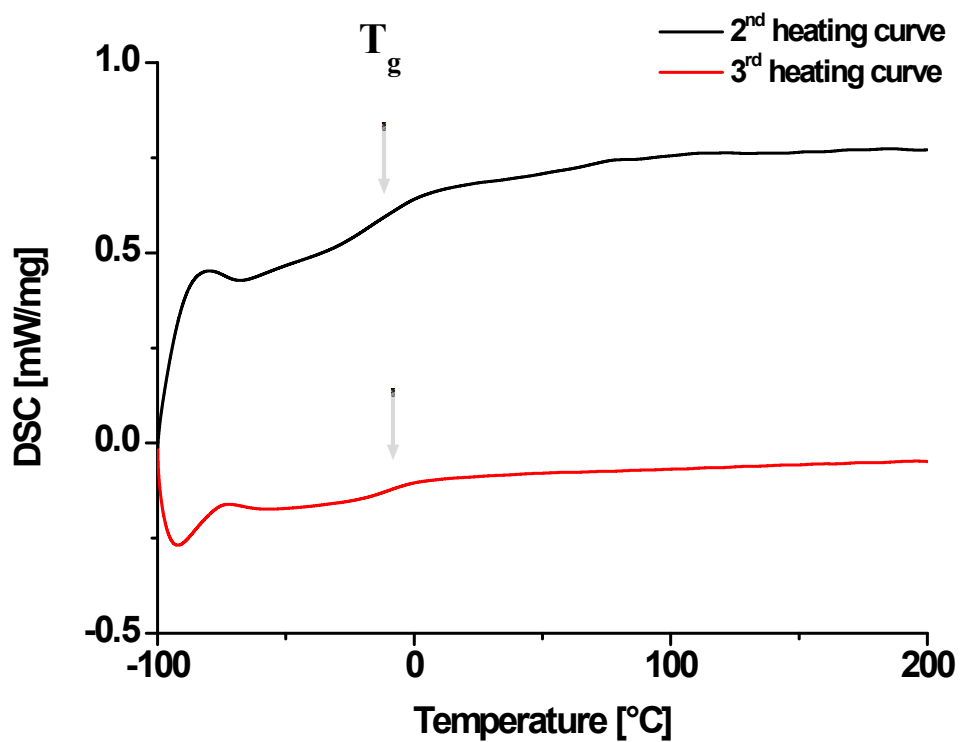


Figure S8: Thermal properties of **P2**. a) DSC curve (2nd heating with 20 K/min and 3rd heating with 10 K/min) and b) TGA curve.

a)



b)

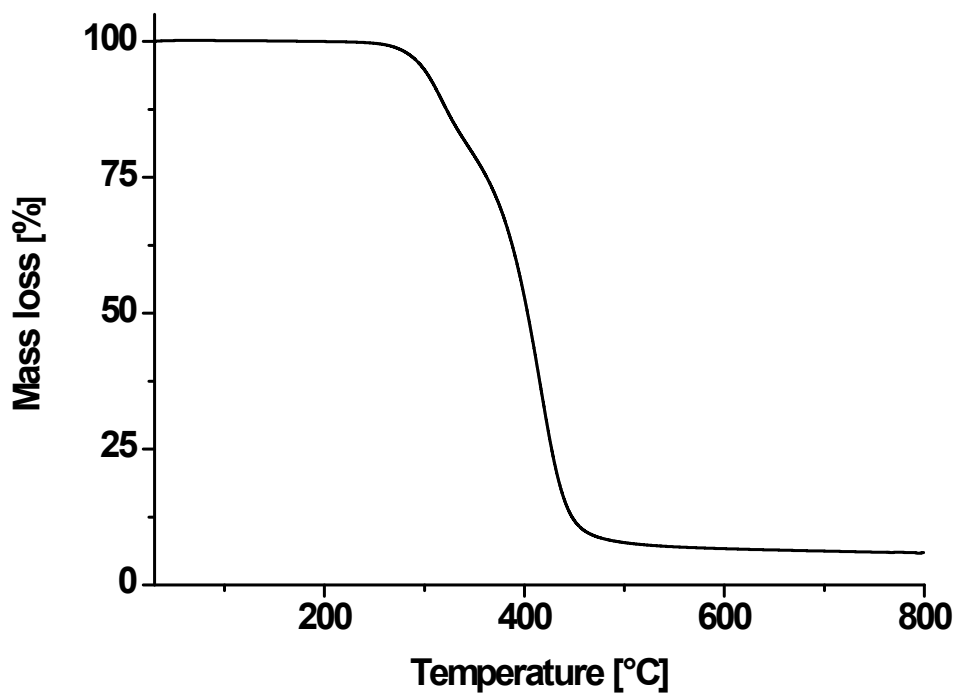
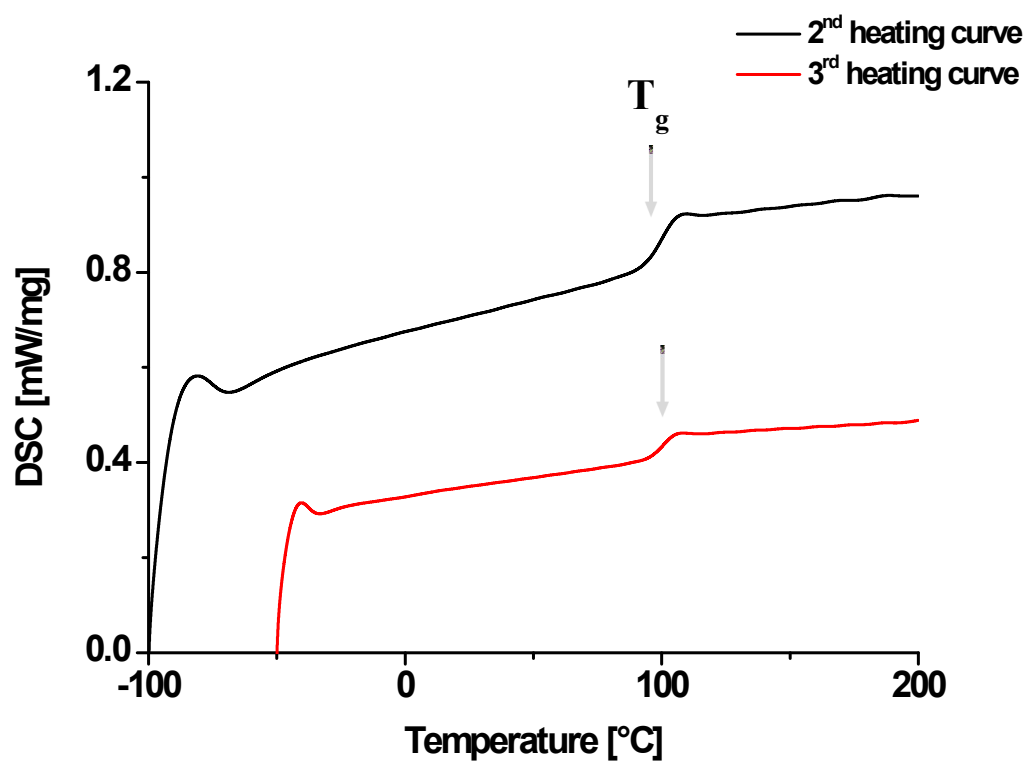


Figure S9: Thermal properties of **P3**. a) DSC curve (2nd heating with 20 K/min and 3rd heating with 10 K/min) and b) TGA curve.

a)



b)

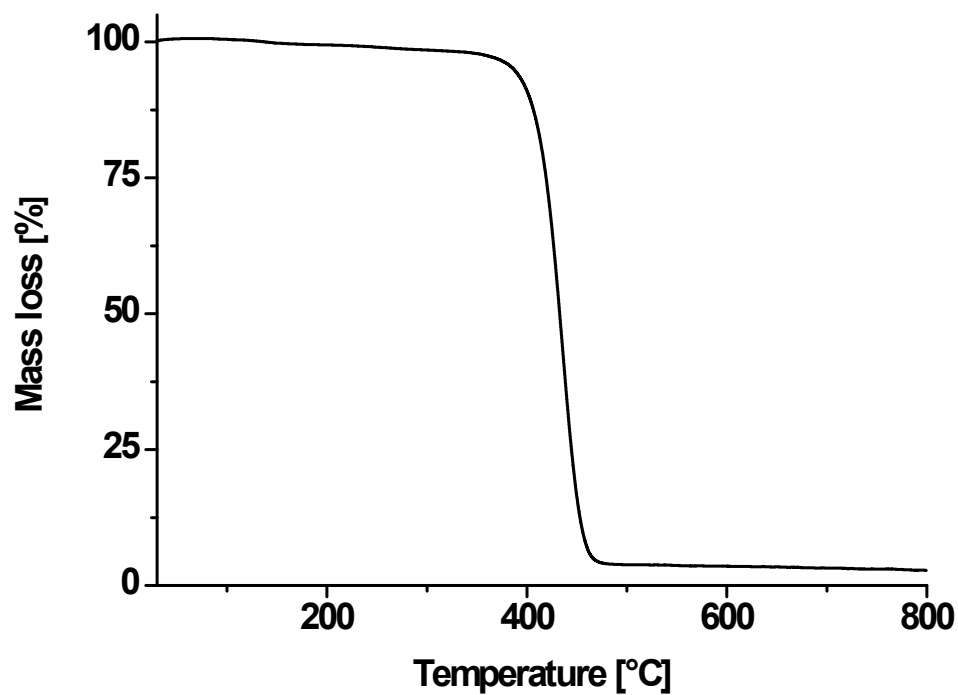
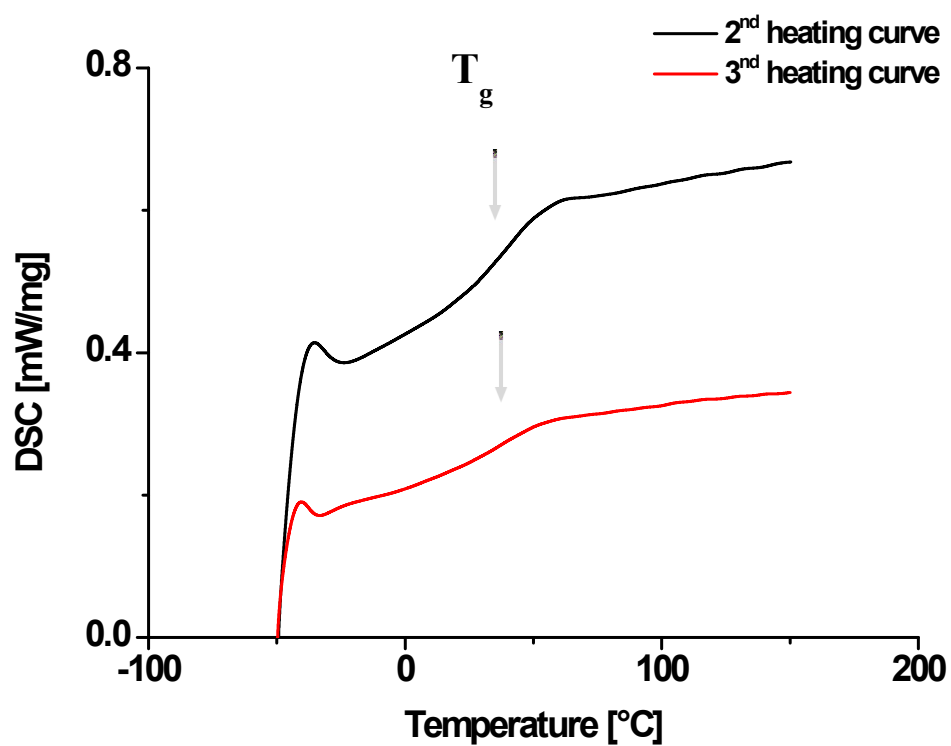


Figure S10: Thermal properties of **P4**. a) DSC curve (2nd heating with 20 K/min and 3rd heating with 10 K/min) and b) TGA curve.

a)



b)

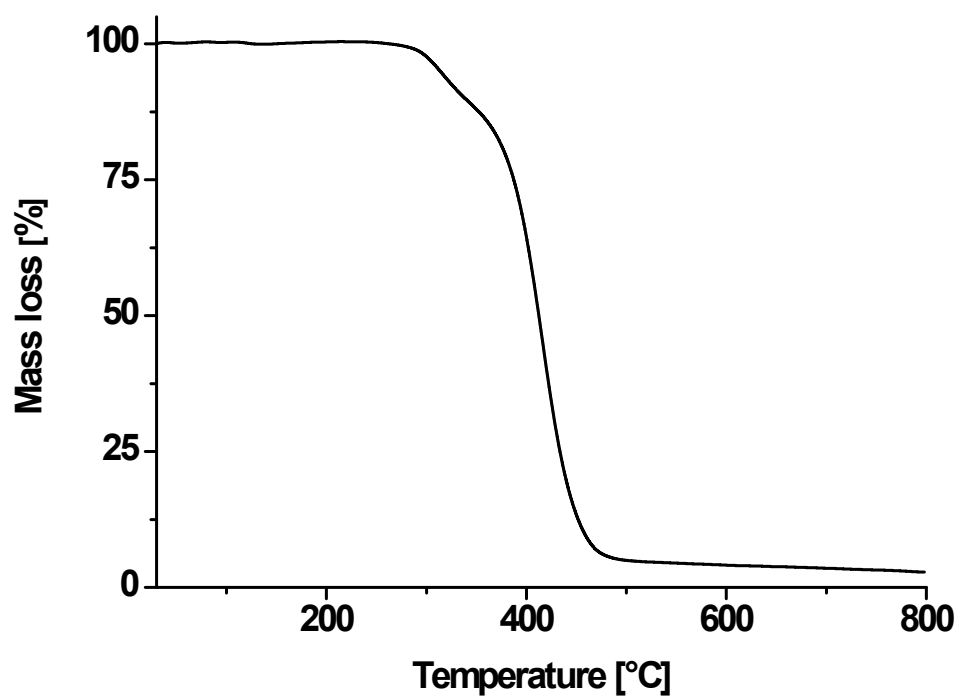
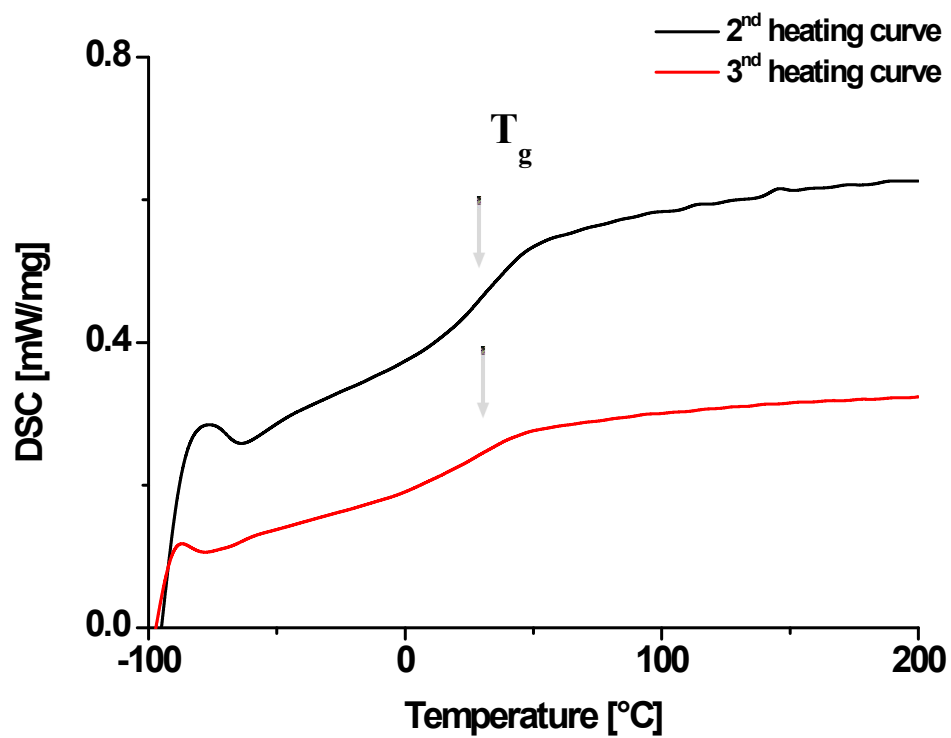


Figure S11: Thermal properties of **P5**. a) DSC curve (2nd heating with 20 K/min and 3rd heating with 10 K/min) and b) TGA curve.

a)



b)

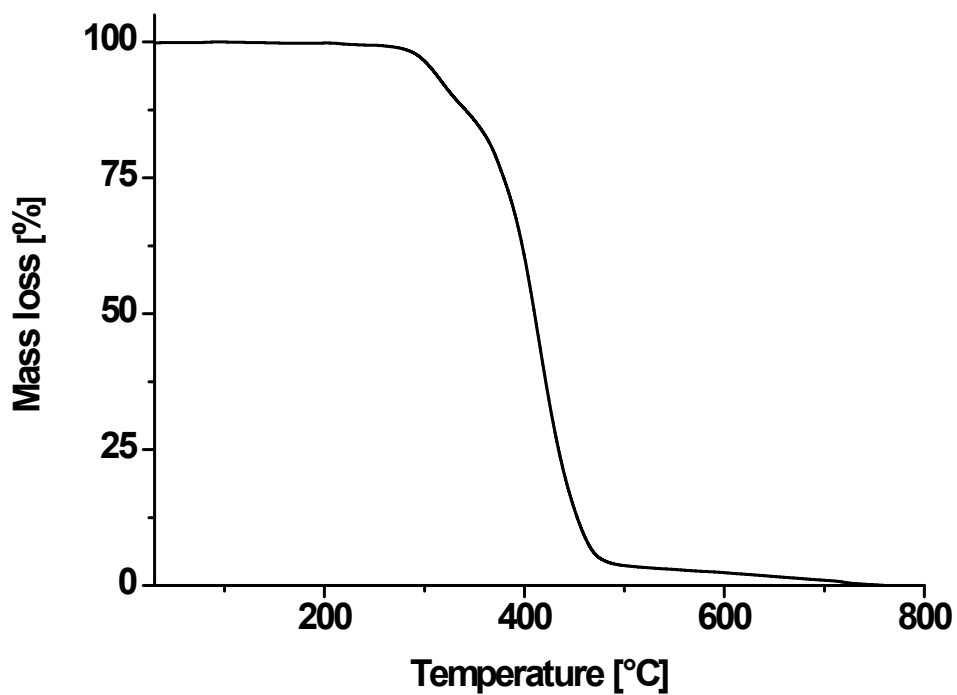
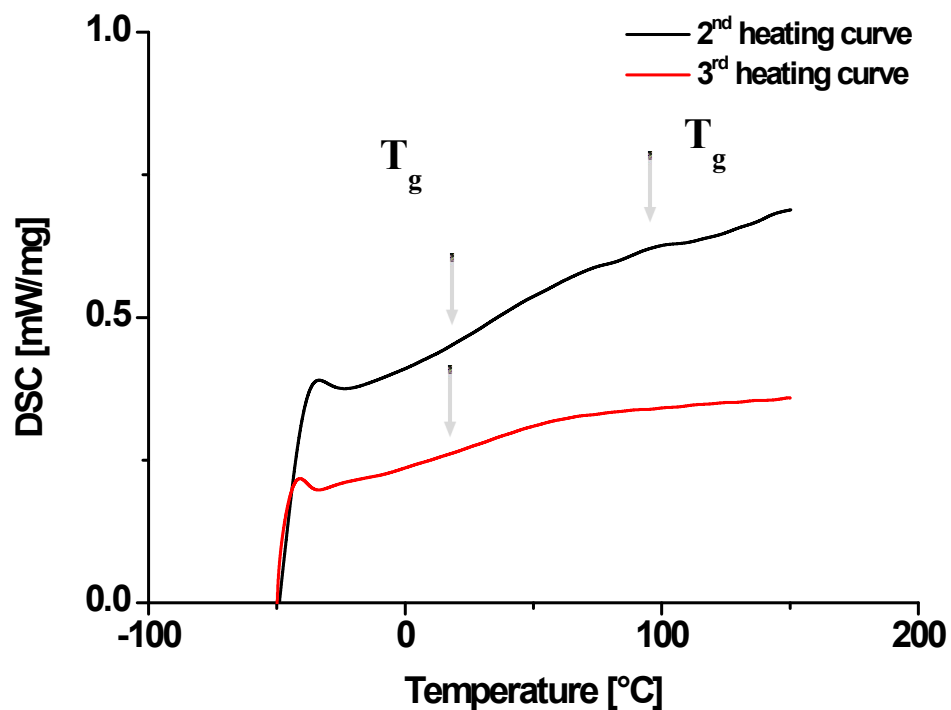


Figure S12: Thermal properties of **P6**. a) DSC curve (2nd heating with 20 K/min and 3rd heating with 10 K/min) and b) TGA curve.

a)



b)

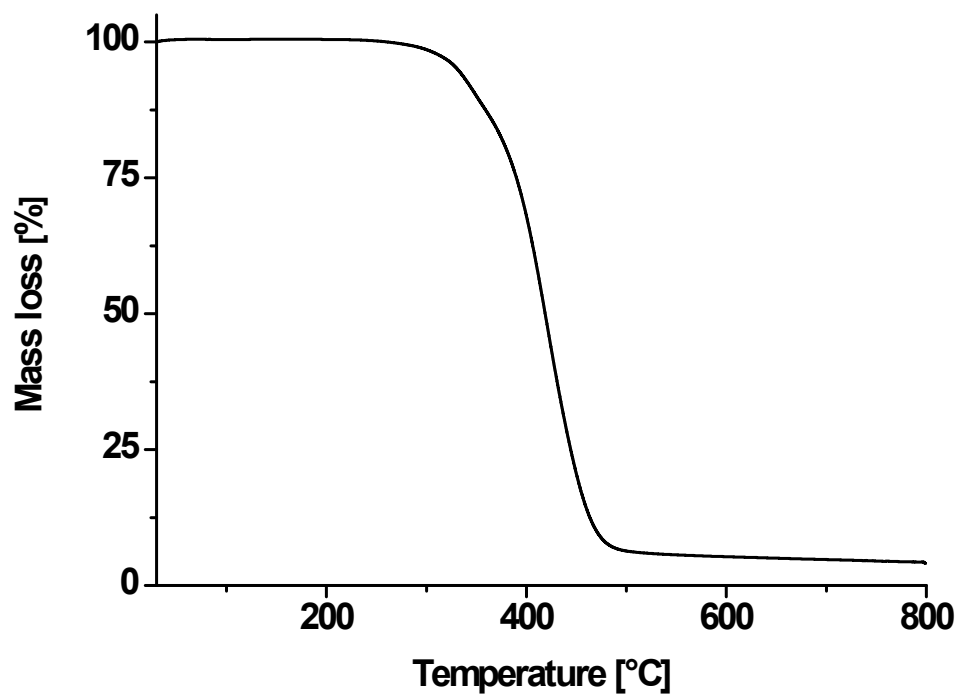
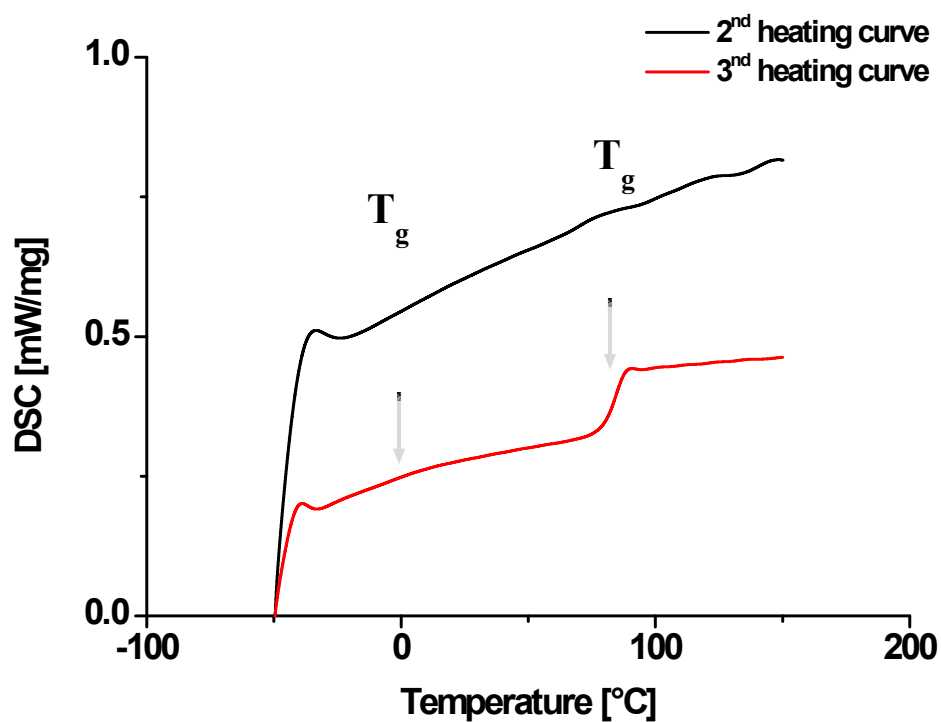


Figure S13: Thermal properties of **P7**. a) DSC curve (hold for 2 h at 50 °C; 2nd heating with 20 K/min and 3rd heating with 10 K/min) and b) TGA curve.

a)



b)

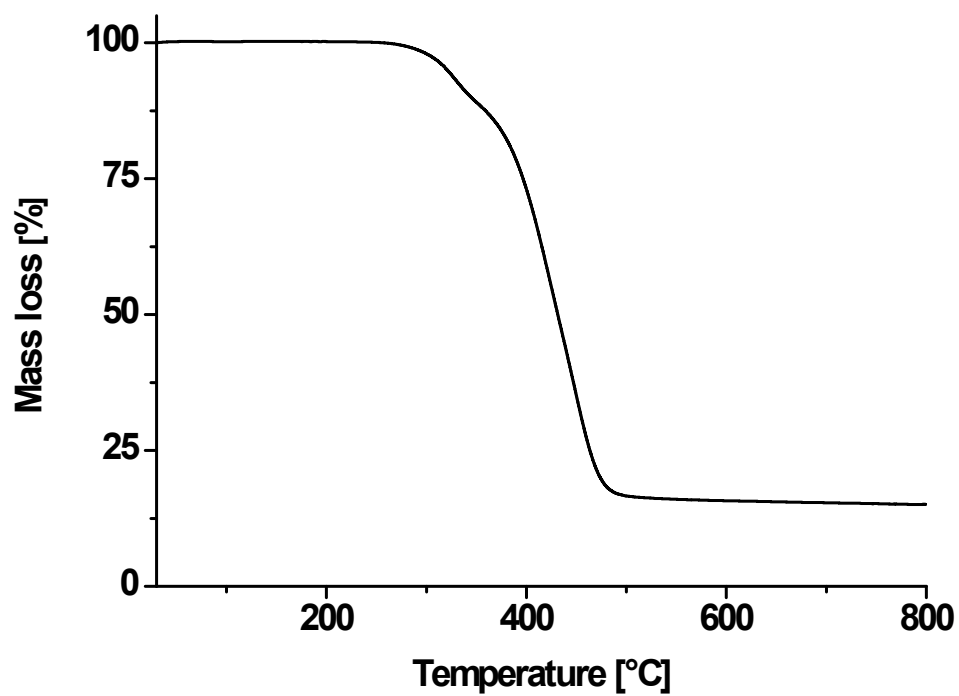


Figure S14: Thermal properties of **P8**. a) DSC curve (hold for 2 h at 50 °C; 2nd heating with 20 K/min and 3rd heating with 10 K/min) and b) TGA curve.

SAXS data of polymers:

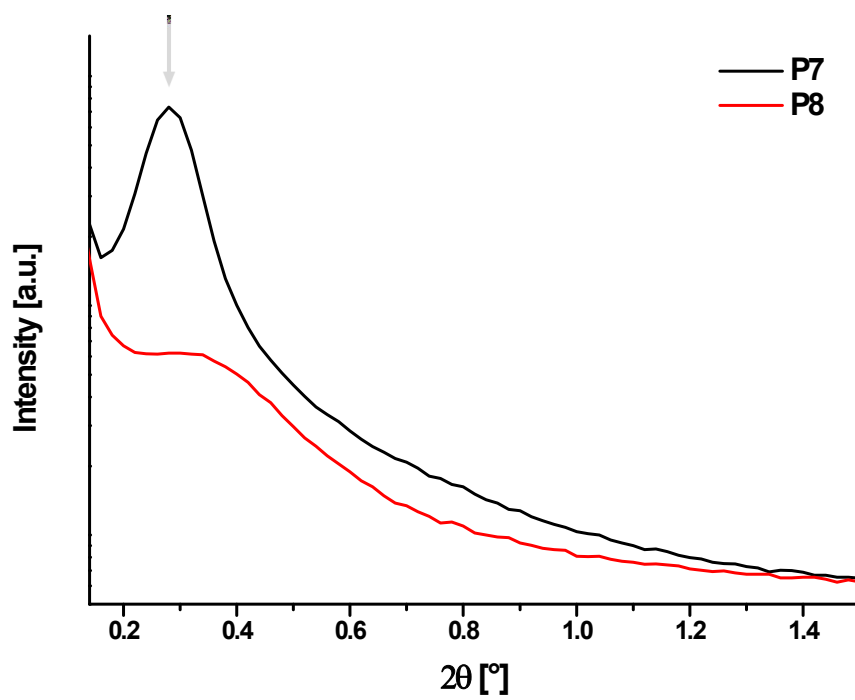
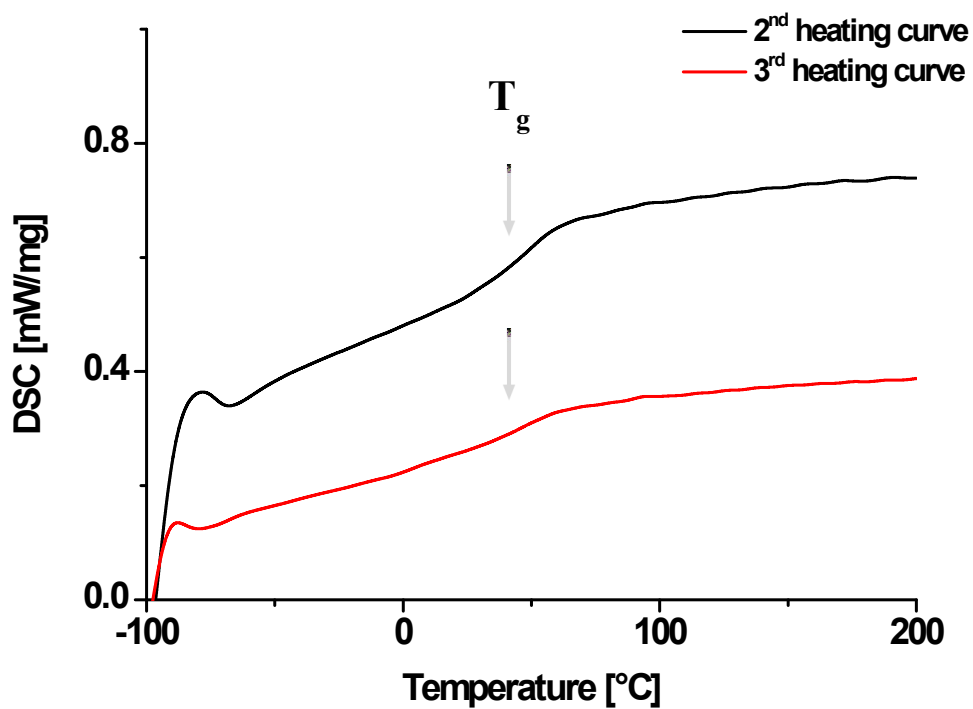


Figure S15: SAXS data of P7 and P8.

DSC/TGA of metallopolymers:

a)



b)

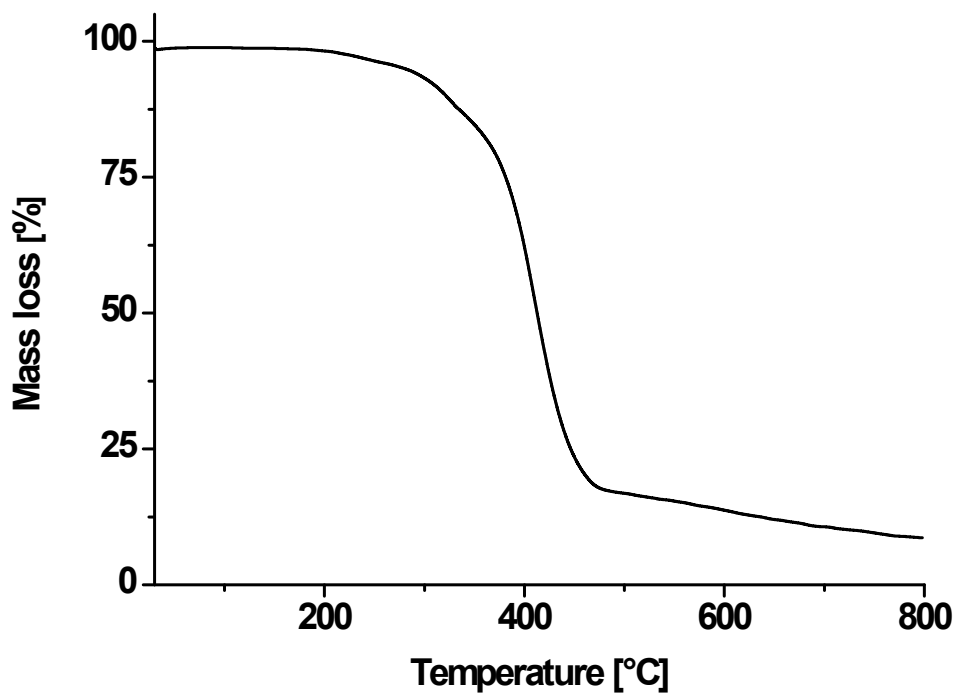
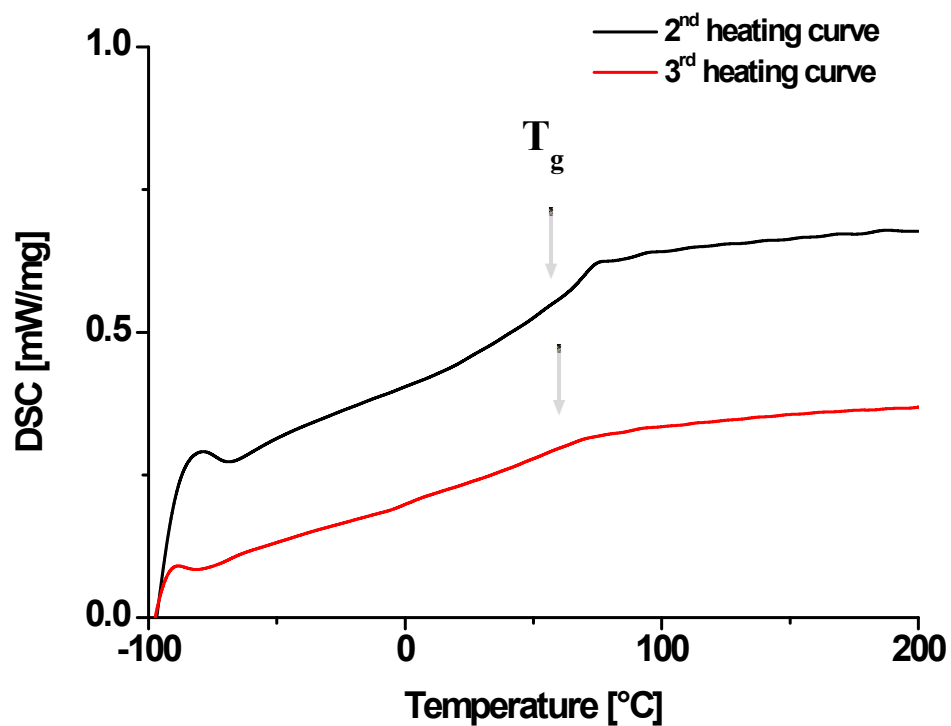


Figure S16: Thermal properties of MP1. a) DSC curve (2nd heating with 20 K/min and 3rd heating with 10 K/min) and b) TGA curve.

a)



b)

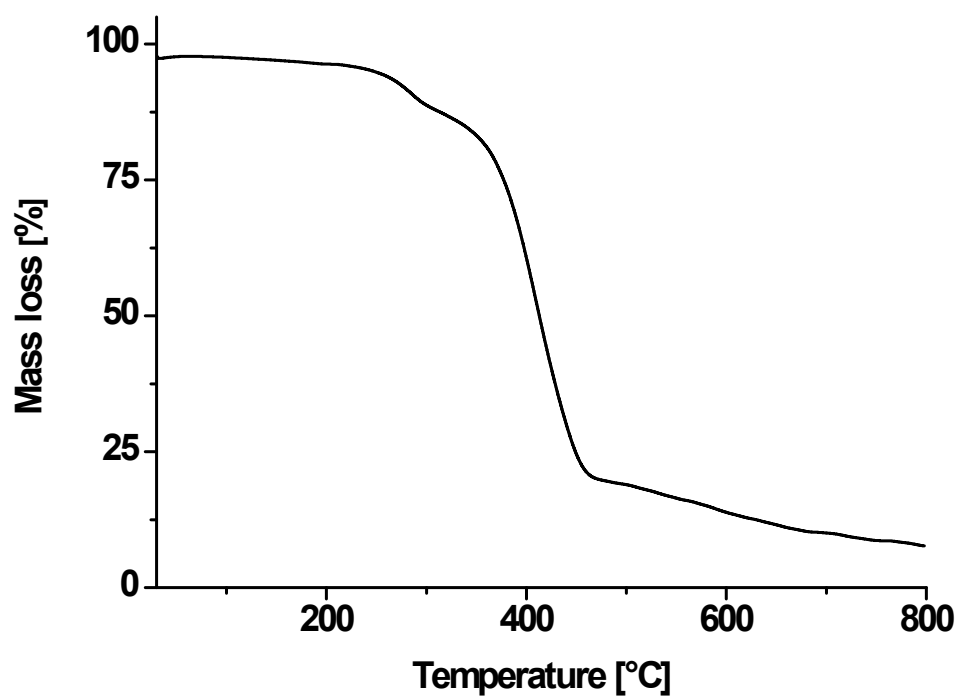
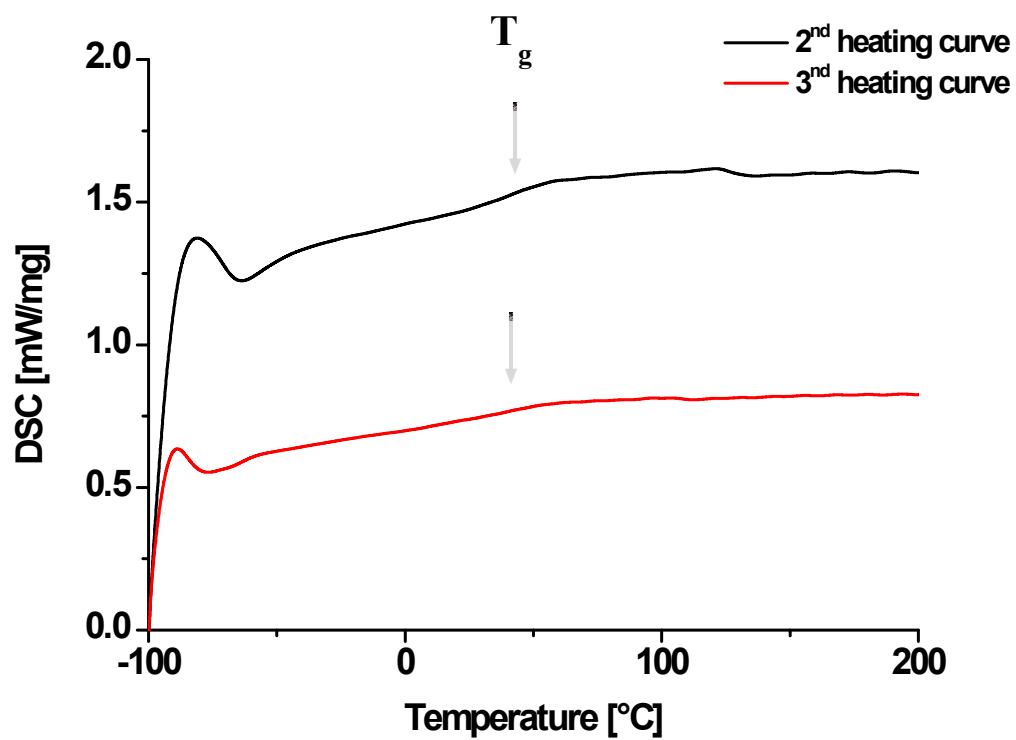


Figure S17: Thermal properties of MP2. a) DSC curve (2nd heating with 20 K/min and 3rd heating with 10 K/min) and b) TGA curve.

a)



b)

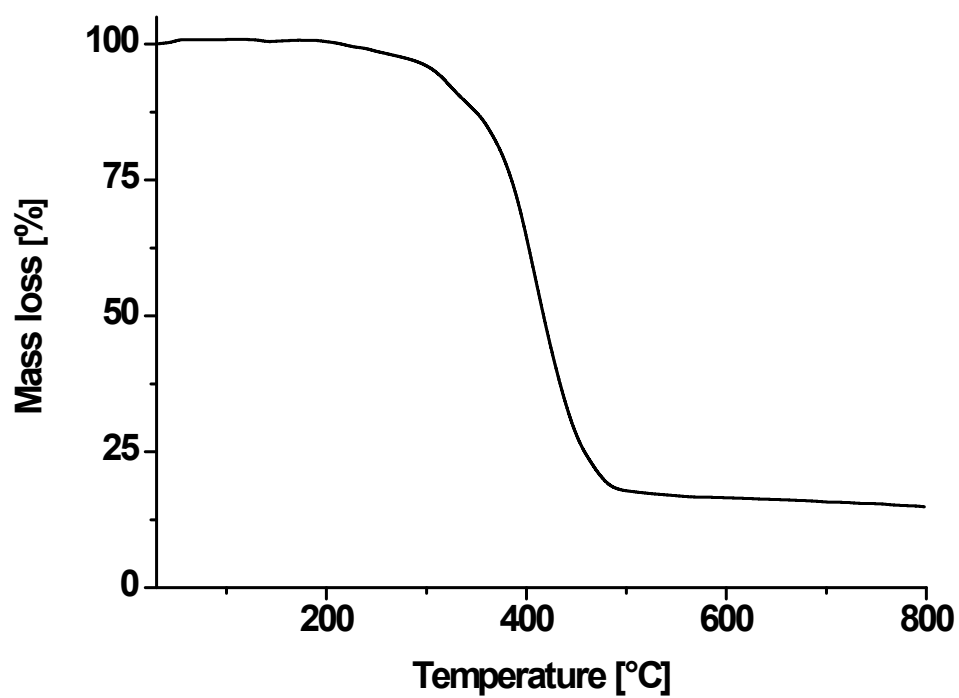
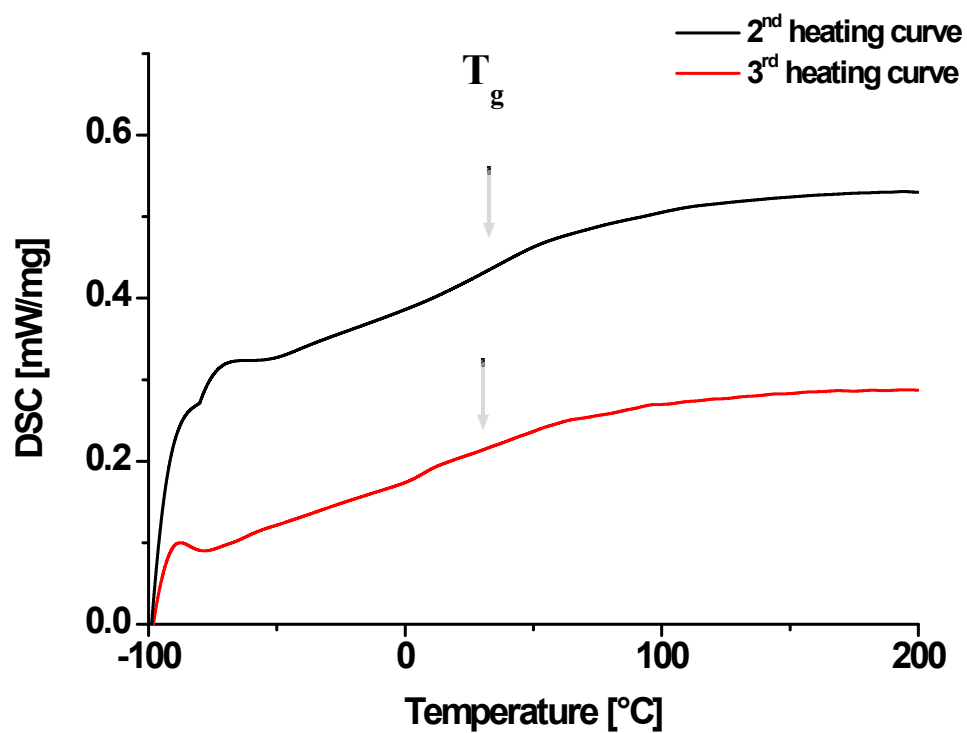


Figure S18: Thermal properties of **MP3**. a) DSC curve (2nd heating with 20 K/min and 3rd heating with 10 K/min) and b) TGA curve.

a)



b)

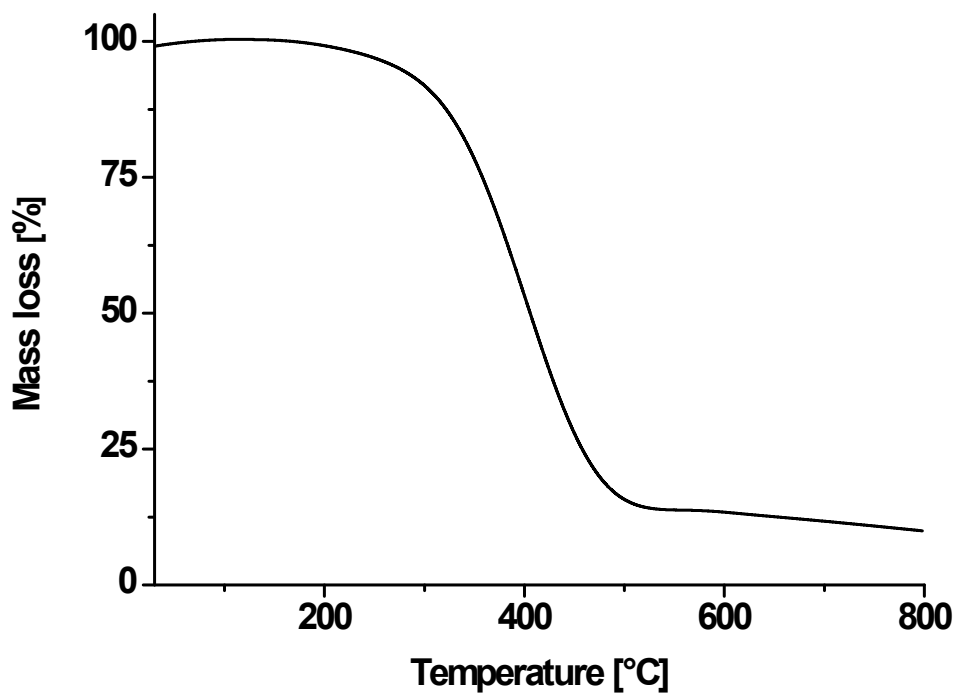
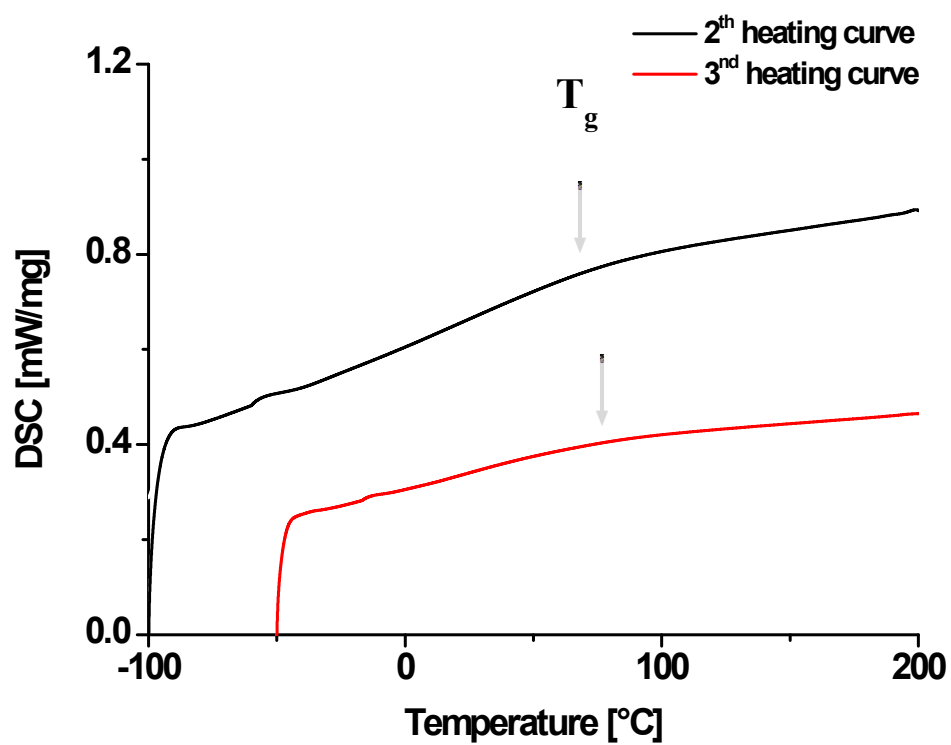


Figure S19: Thermal properties of MP4. a) DSC curve (2nd heating with 20 K/min and 3rd heating with 10 K/min) and b) TGA curve.

a)



b)

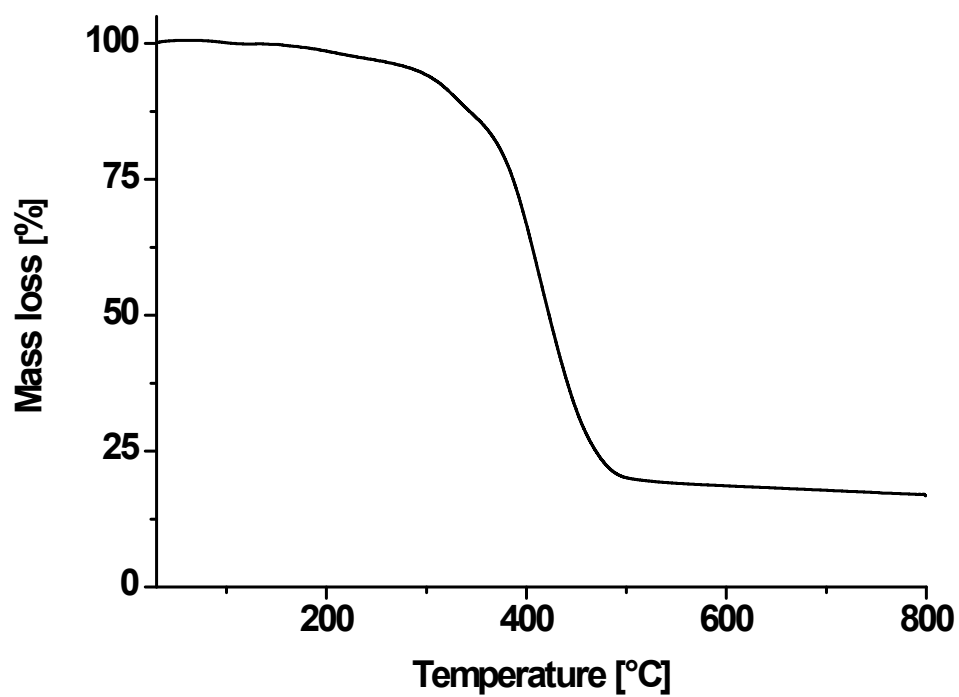
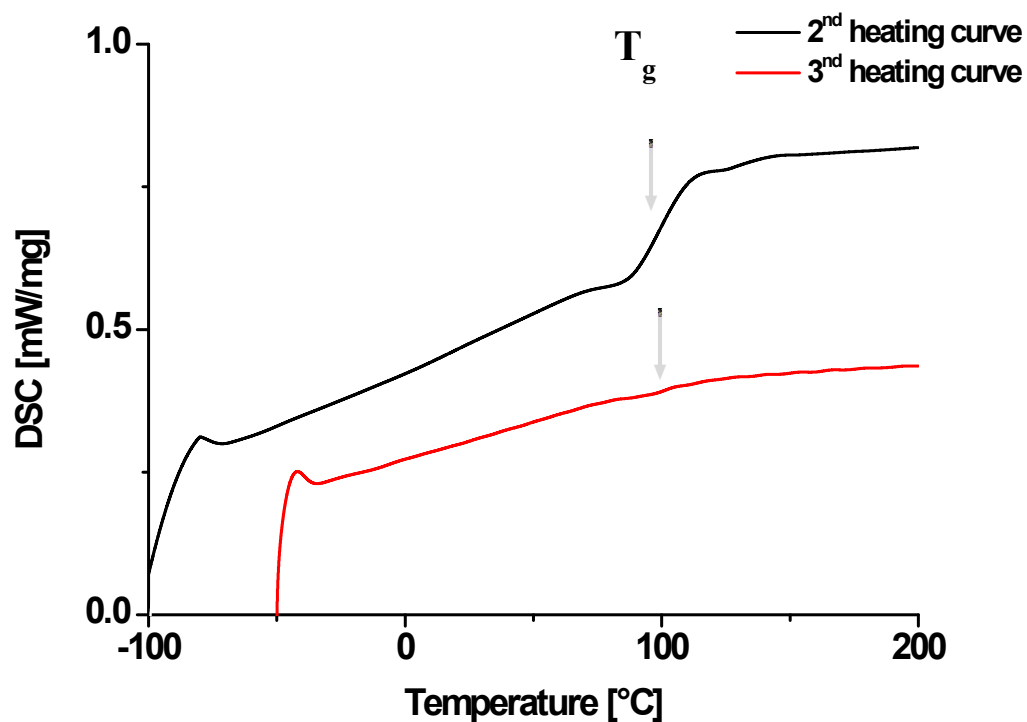


Figure S20: Thermal properties of MP5. a) DSC curve (2nd heating with 20 K/min and 3rd heating with 10 K/min) and b) TGA curve.

a)



b)

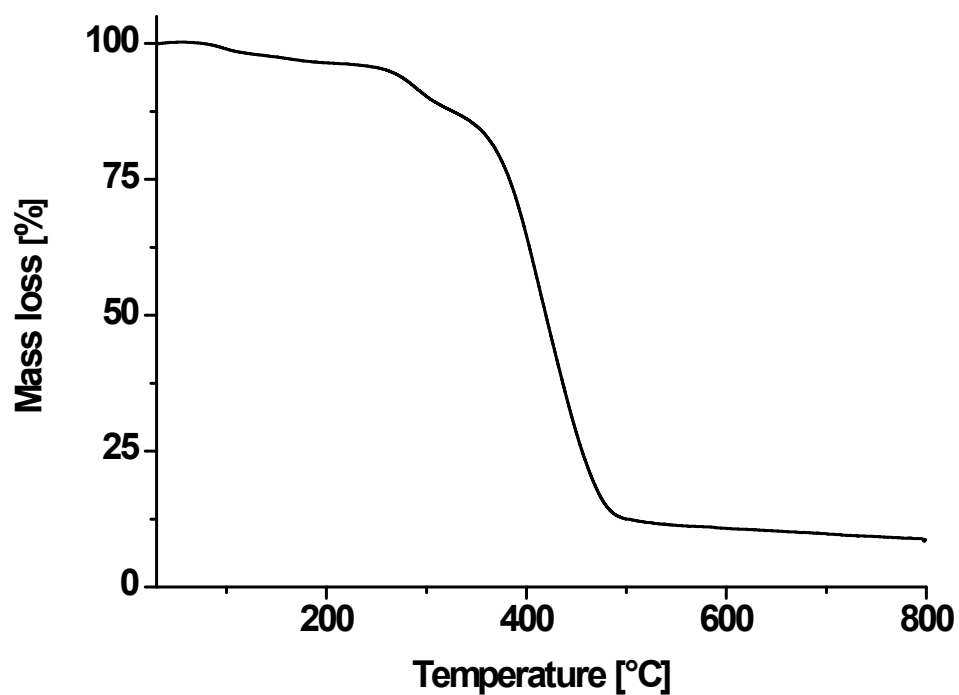
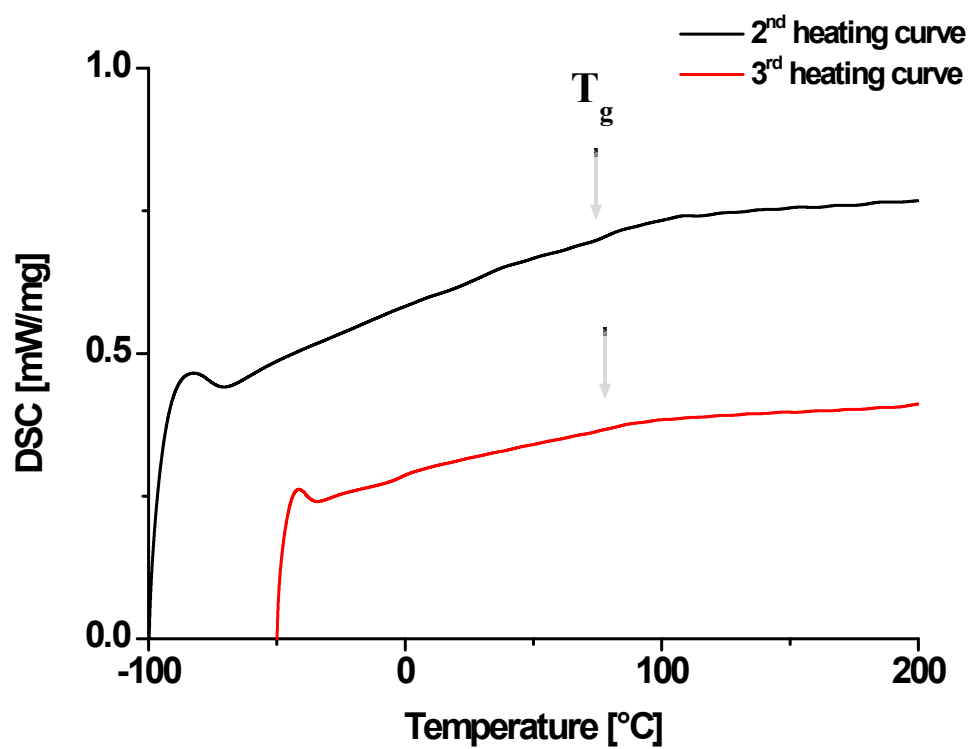


Figure S21: Thermal properties of MP6. a) DSC curve (2nd heating with 20 K/min and 3rd heating with 10 K/min) and b) TGA curve.

a)



b)

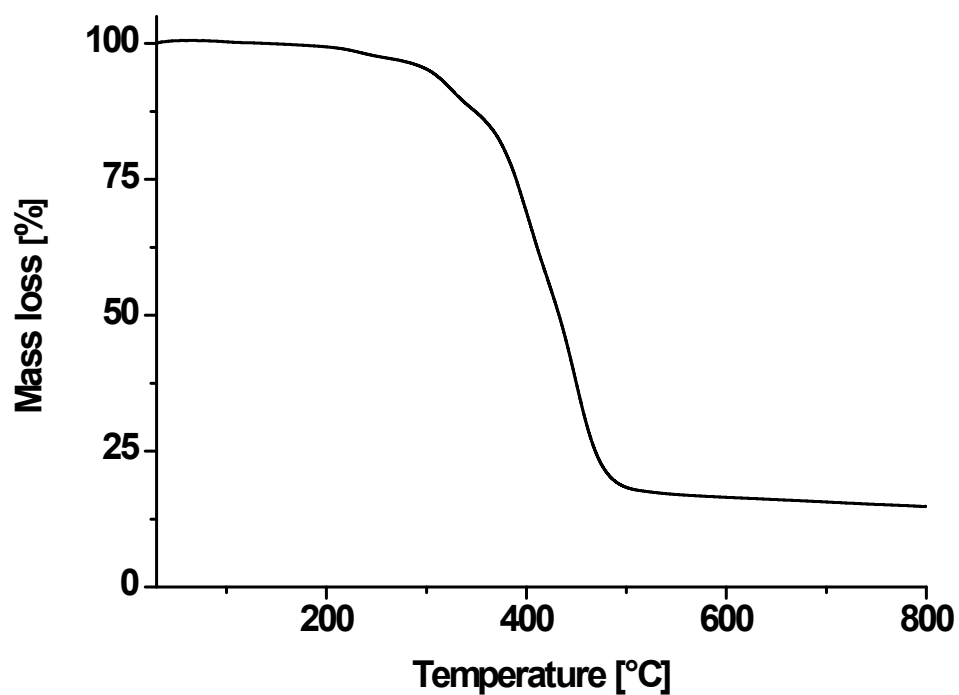
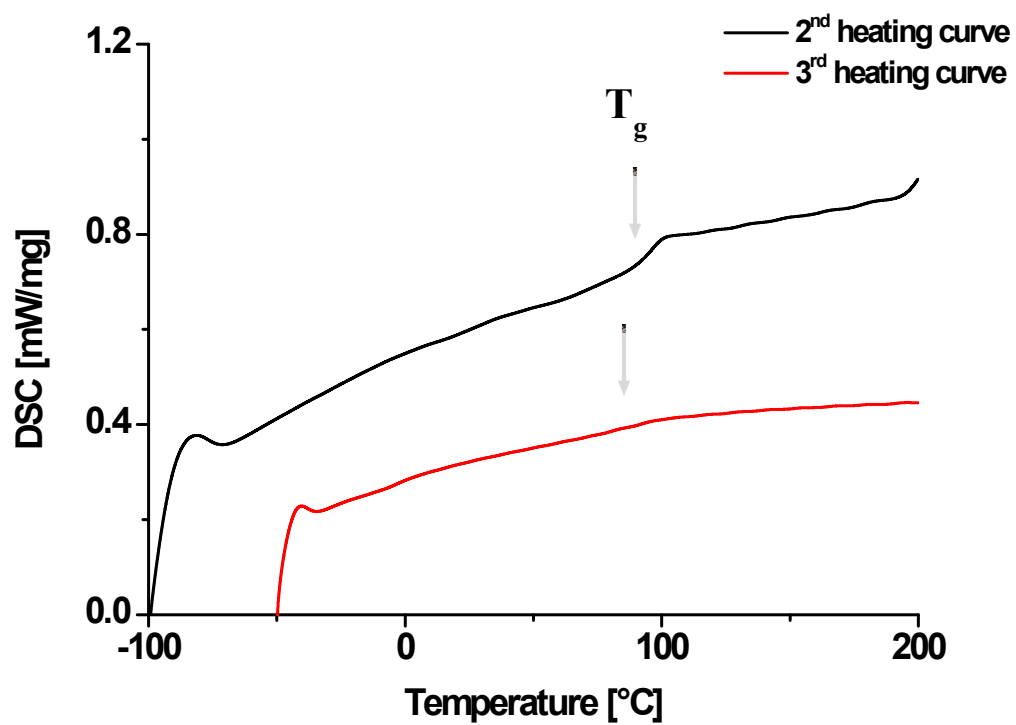


Figure S22: Thermal properties of MP7. a) DSC curve (2nd heating with 20 K/min and 3rd heating with 10 K/min) and b) TGA curve.

a)



b)

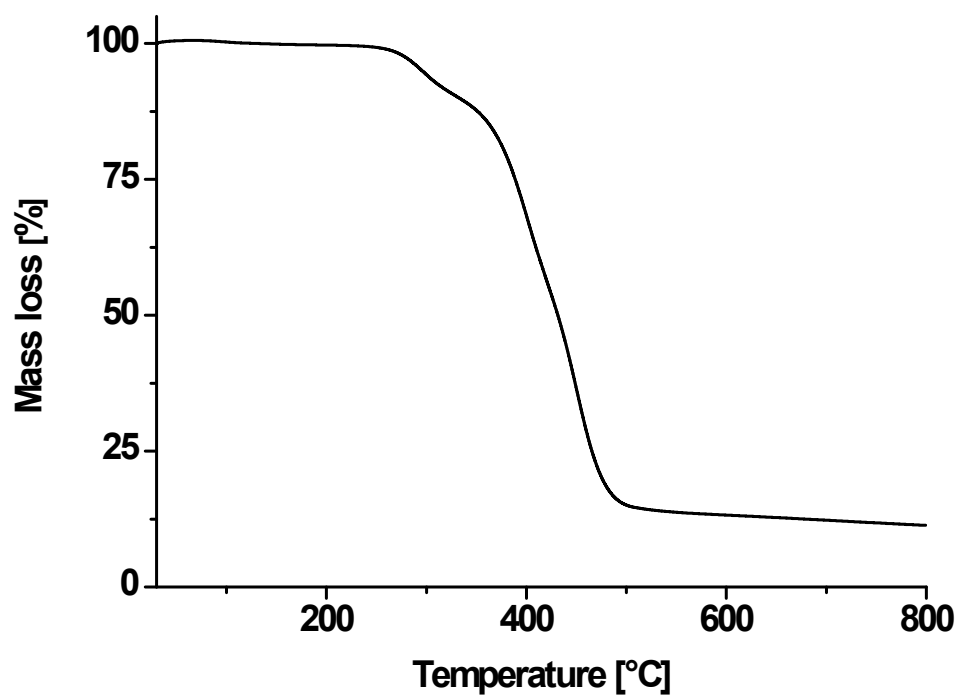


Figure S23: Thermal properties of MP8. a) DSC curve (2nd heating with 20 K/min and 3rd heating with 10 K/min) and b) TGA curve.

SAXS data of metallopolymers:

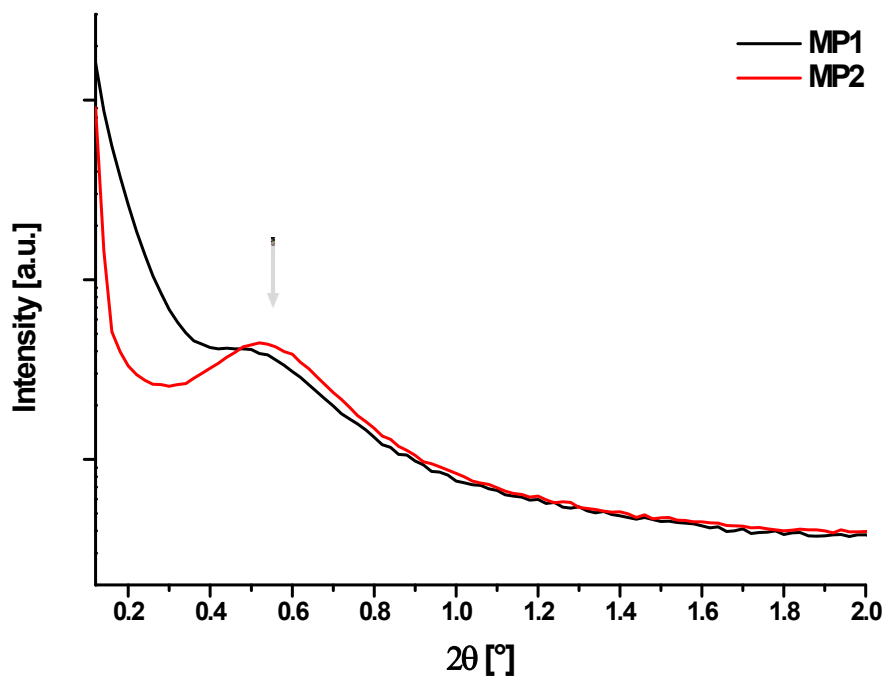


Figure S24: SAXS data of **MP1** and **MP2** (SAXS data of **MP3** and **MP4** show no reflex and thus are not depicted).

Self-healing tests:

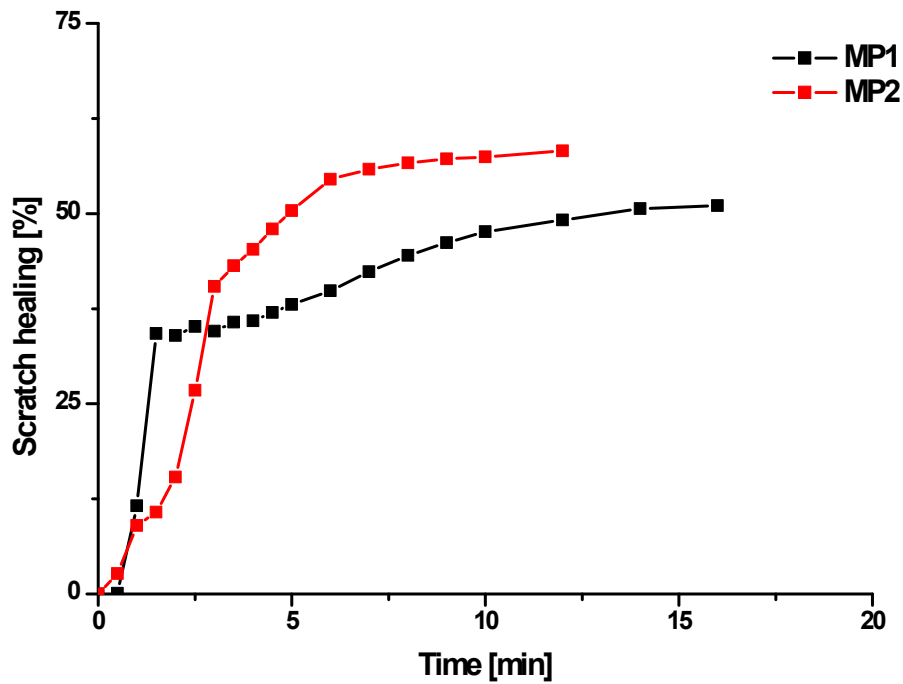


Figure S25: Quantitative scratch surface recovery at 100 °C of (a) MP1 and (b) MP2.

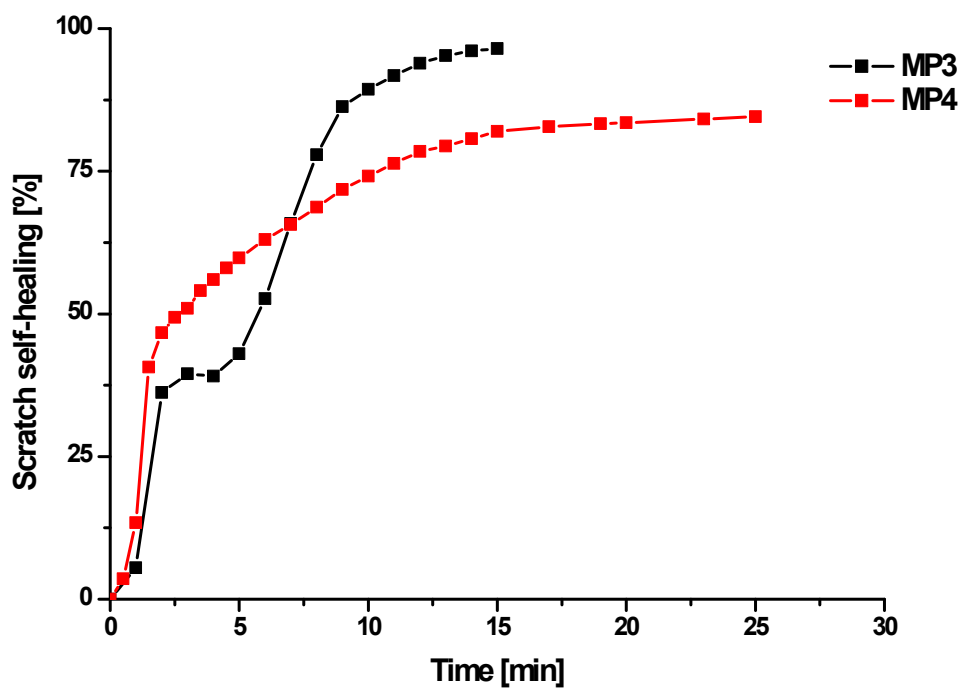


Figure S26: Quantitative scratch surface recovery at 100 °C of (a) MP3 and (b) MP4.

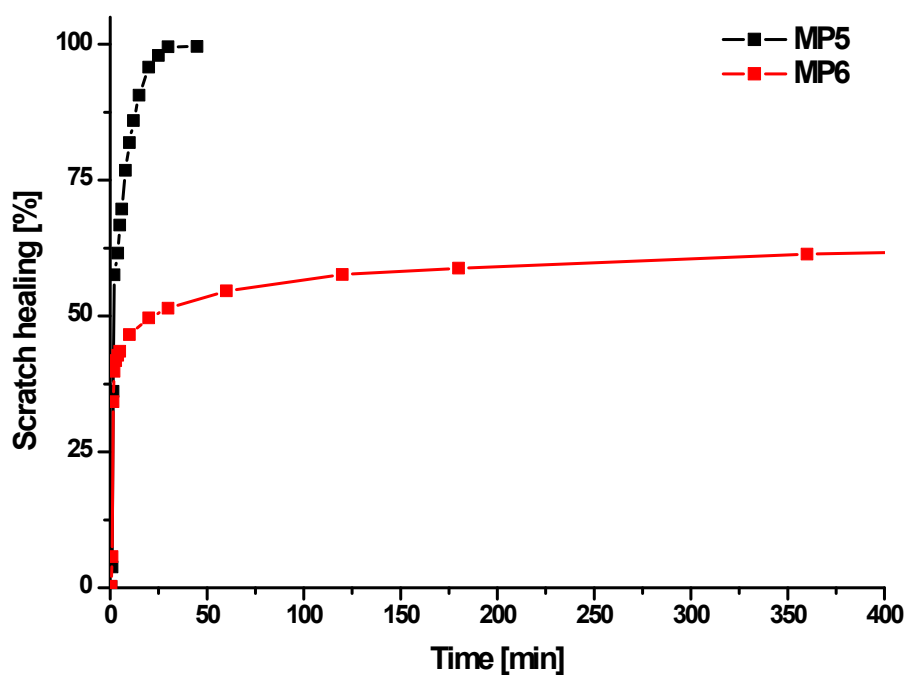


Figure S27: Quantitative scratch surface recovery at 100 °C of (a) MP5 and (b) MP6.

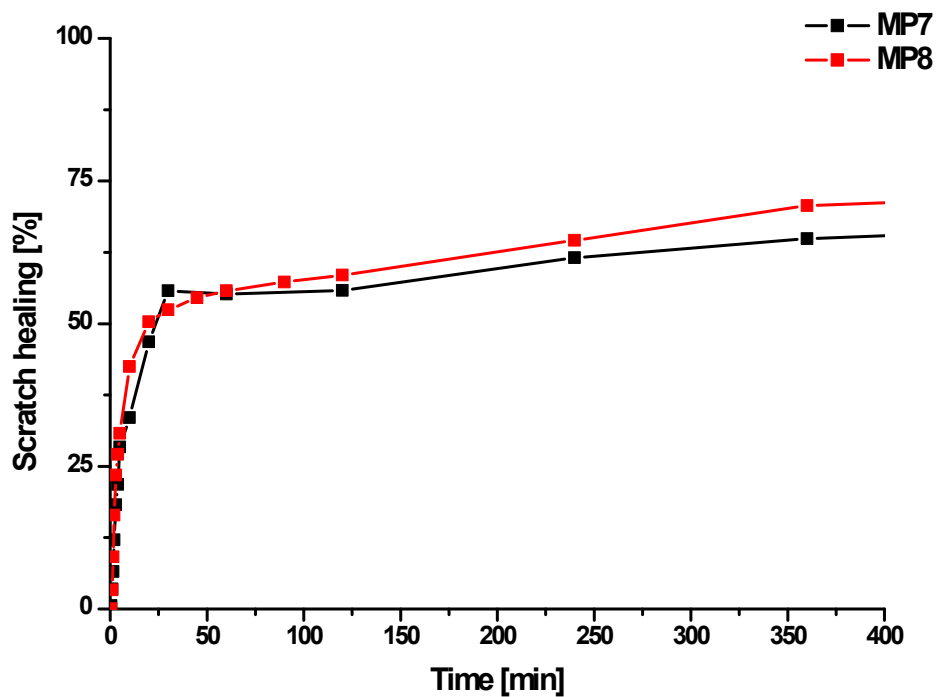


Figure S28: Quantitative scratch surface recovery at 100 °C of (a) MP7 and (b) MP8.

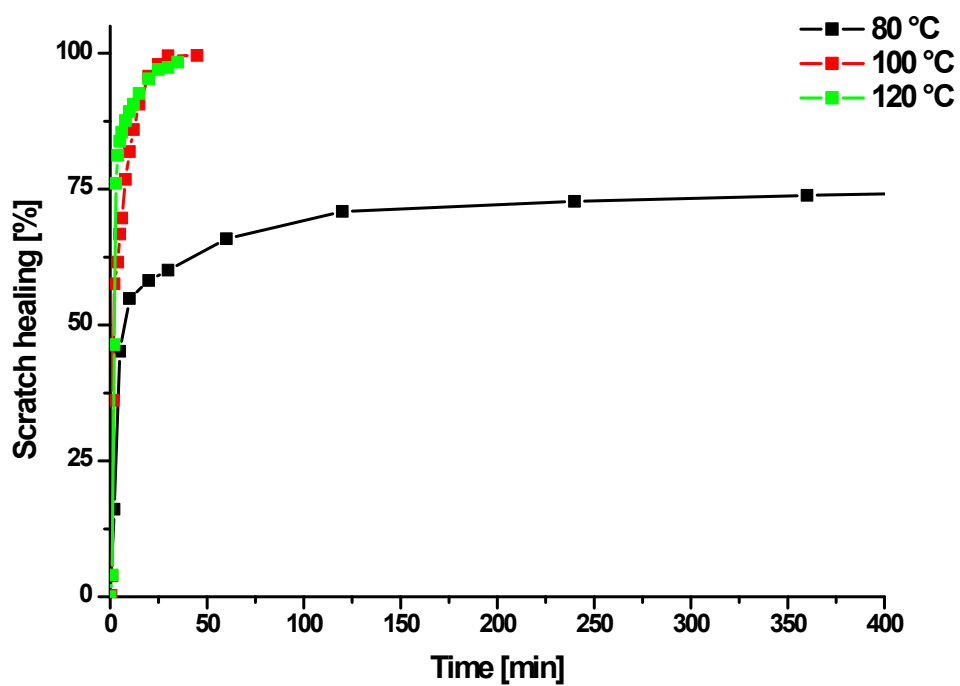


Figure S29: Quantitative scratch surface recovery of **MP5** at different temperatures.

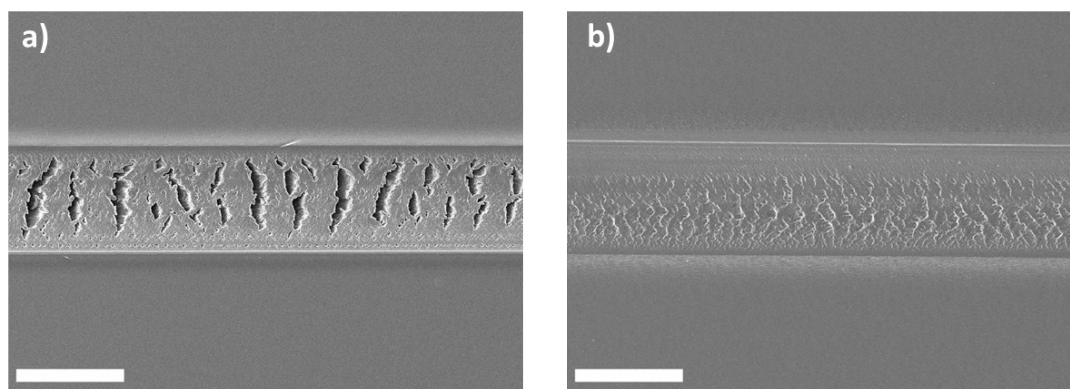
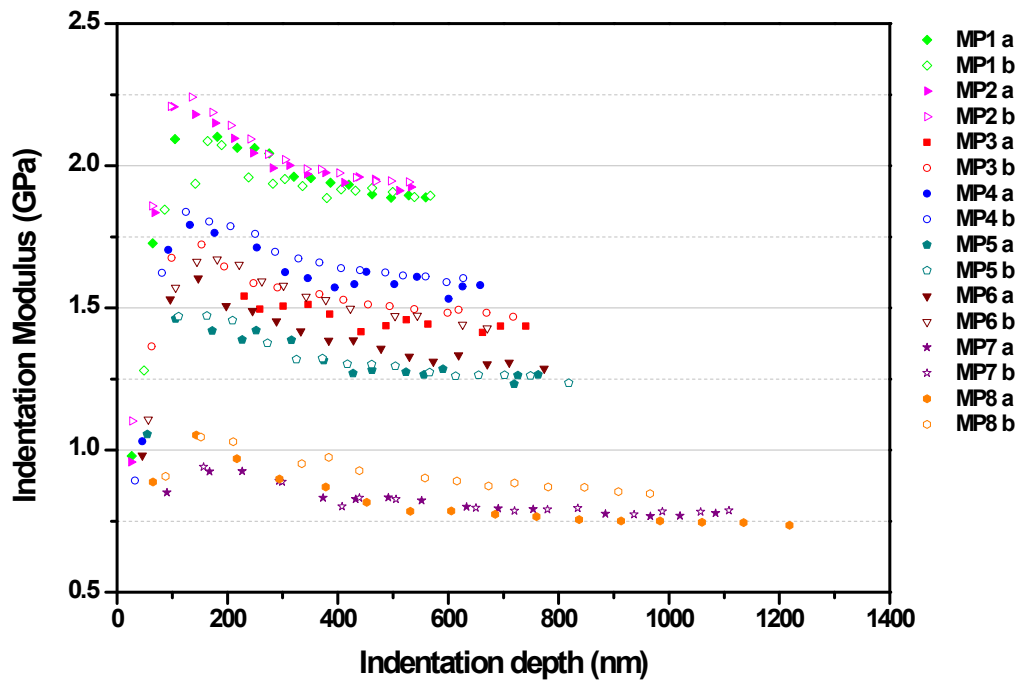


Figure S30: Scanning electron microscopy (SEM) images of the shape of the scratches of **MP5** (a) and **MP8** (b). Scale bars are 100 μm .

Nanoindentation:

a)



b)

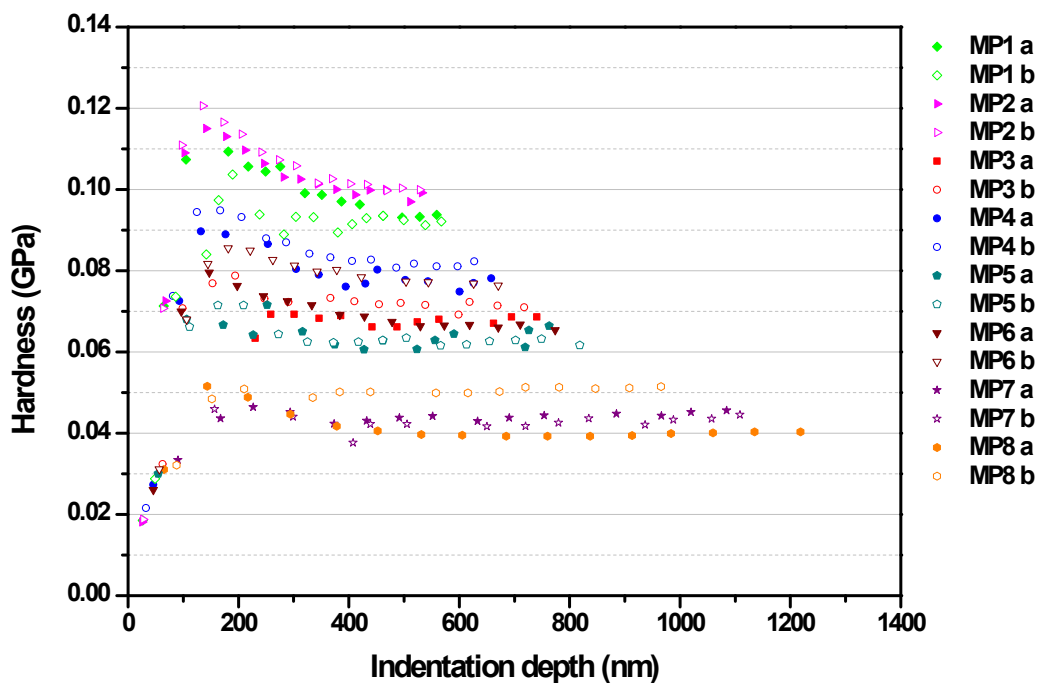


Figure S31: Mechanical properties measured by nanoindentation of **MP1** to **MP8**. a) Indentation modulus and b) hardness (measurements were repeated in two measuring areas (a and b of sample name) with sixteen maximum loads in a 4×4 array).

Tables:**Table S1:** Summary of the SEC results (eluent: DMAc + 0.21% LiCl) and thermal properties of the polymers **P1** to **P8** and resulting ratios of *n*-butyl acrylate (BA) and **1** calculated from ¹H NMR.

Sample	M _{n,SEC} [g/mol]	M _{w,SEC} [g/mol]	Đ	Hard vs. soft block _{NMR}	Ratio _{NMR} [1]:[BA]	DSC: T _g [°C]	TGA: T _d [°C]
P1	9,900 ^a	12,400	1.25	–	1:10	–19.2	288
P2	8,900 ^b	11,100	1.25	–	–	94.7	346
P3	24,900 ^a	32,400	1.30	–	1:10	–4.6	299
P4	22,400 ^b	28,700	1.28	–	–	100.0	387
P5	17,200 ^a 16,800 ^b	21,800 20,900	1.27 1.25	1:1	1:10	36.3	314
P6	15,100 ^a 14,900 ^b	19,500 18,800	1.29 1.26	1:1	1:10	31.1	308
P7	43,800 ^a 41,500 ^b	66,200 61,100	1.51 1.47	1:1	1:10	22.1 + 93.7	331
P8	36,100 ^a 34,600 ^b	54,200 50,300	1.50 1.45	1:1	1:10	5.1 + 83.7	321

a = PMMA standard, b = PS standard.

Table S2: Overview of the elemental analysis results of metallopolymers **MP1** to **MP8**.^a

Metallo-polymer	Used polymer	Metal salt	Carbon [%]	Hydrogen [%]	Nitrogen [%]	Chloride [%]
MP1	P5	Zn(OAc) ₂	78.66	8.15	1.59	–
MP2	P5	ZnCl ₂	76.30	7.76	1.56	3.65
MP3	P6	Zn(OAc) ₂	78.43	8.32	1.79	–
MP4	P6	ZnCl ₂	76.69	7.97	1.81	1.96
MP5	P7	Zn(OAc) ₂	75.84	7.84	1.57	–
MP6	P7	ZnCl ₂	78.37	8.11	1.63	1.16
MP7	P8	Zn(OAc) ₂	78.24	8.17	1.74	–
MP8	P8	ZnCl ₂	78.28	8.15	1.76	1.61

a = TGA measurements (**Figure S16** to **Figure S23**) indicated that at 800 °C approximately 8% to 17% of material is remaining. Thus, the exact metal content cannot be calculated from elemental analysis and TGA, respectively.

Table S3: SAXS results of the block copolymers **P5** to **P8** and the metallopolymers **MP1** to **MP8**.

Material	SAXS [2θ in $^\circ$]	Domain size [nm]
P5	— ^a	—
P6	— ^a	—
P7	0.28	— ^b
P8	0.28	— ^b
MP1	0.50	— ^b
MP2	0.52	— ^b
MP3	— ^a	—
MP4	— ^a	—
MP5	0.38	— ^b
MP6	0.38	— ^b
MP7	0.28, 0.62	31.5
MP8	0.28, 0.62	31.5

a = No SAXS-reflex observed, b = Broad signal - disordered

The domain size was calculated with the following equation (Bragg's law):

$$d = \frac{n\lambda}{2 \sin(\frac{2\theta}{2})} \quad (1)$$

d = interplanar distance, n = positive integer, λ = wavelength, θ = scattering angle

Table S4: Depth-sensing indentation (DSI) results (combined results from two measuring areas of the same sample).

Sample	M.-points ^a	Reduced modulus E_r ^{b, c}		Hardness ^{b, c}		Indentation modulus E_i ^d	
		Average ^a	Standard deviation	Average ^a	Standard deviation	Average ^a	Standard deviation
		N	GPa	GPa	GPa	GPa	GPa
MP1	27	2.329	0.087	0.096	0.006	1.960	0.073
MP2	27	2.410	0.115	0.105	0.006	2.029	0.097
MP3	25	1.788	0.085	0.070	0.003	1.504	0.071
MP4	27	1.967	0.099	0.083	0.006	1.655	0.084
MP5	29	1.574	0.091	0.064	0.003	1.324	0.077
MP6	27	1.743	0.140	0.074	0.007	1.466	0.118
MP7	27	0.974	0.061	0.043	0.002	0.819	0.051
MP8	28	1.025	0.114	0.046	0.005	0.861	0.096

^a Measurements were repeated in two measuring areas with sixteen maximum loads in a 4×4 array, increasing in steps of 100 μN from 100 μN to 1600 μN . Values are averaged, measurements outside the area function limits of 150 to 2000 nm were excluded. ^b The depth-sensing indentation (DSI) was conducted at ambient conditions at 23.7 ± 0.8 °C and $22.4 \pm 4.3\%$ relative humidity (RH). ^c For quasi-static testing, a 5 s loading, 20 s hold at maximum load, and 5 s unloading profile was applied. ^d From the reduced modulus E_r , the indentation modulus E_i was calculated using the analysis method proposed by Oliver and Pharr, using the elastic modulus and Poisson's ratio of the diamond indenter, 1140 GPa and 0.07, respectively, and a Poisson's ratio of 0.4 for the polymeric material.^[S5]

Experimental section

Table S5: Overview of the reaction details of the RAFT polymerizations (**P1** to **P8**) [DBTTC = S,S-dibenzyl trithiocarbonate; BA = n-butyl acrylate].

Sample	Monomers	m (monomer) [g]	m (AIBN) [mg]	m (CTA) [mg]	[M]/[CTA] ratio	V (solvent) [mL]
P1	1	0.81	8.29	DBTTC	85/1	8.58
	BA	2.00		58.66		
P2	Styrene	5.00	3.03	DBTTC 21.45	650/1	12.00
P3	1	0.89	2.92	DBTTC	265/1	9.44
	BA	2.2		20.70		
P4	Styrene	15.00	2.37	DBTTC 16.73	2500/1	36.01
P5	Styrene	3.05	3.76	P1 915.15	320/1	14.69
P6	1	0.26	2.61	P2	85/1	2.74
	BA	0.63		636.10		
P7	Styrene	8.87	1.76	P3 1070.02	1990/1	21.30
P8	1	0.57	2.41	P4	205/1	6.06
	BA	1.41		1470.51		

Analysis of the polymers:

P1

¹H NMR (300 MHz, CD₂Cl₂): δ = 0.74 – 2.53 (112H), 2.67 – 3.32 (4H), 3.81 – 4.20 (20H), 4.37 – 4.64 (1H), 6.61 – 6.72 (1H), 6.97 – 7.51 (16H) ppm.

SEC (DMAc + 0.21% LiCl, PMMA-standard): M_n = 9,900 g/mol; M_w = 12,400 g/mol; \bar{D} = 1.25

EA: (calcd. for repeating units based on NMR)

calcd.: C: 68.64%; H: 8.72%; N: 3.11%

found: C: 68.55%; H: 8.67%; N: 3.08%

DSC: T_g : -19 °C; TGA: T_d : 288 °C

P2

¹H NMR (300 MHz, CD₂Cl₂): δ = 1.26 – 2.46 (3H), 6.36 – 7.40 (5H) ppm.

SEC (DMAc + 0.21% LiCl, PS-standard): M_n = 8,900 g/mol; M_w = 11,100 g/mol; Đ = 1.25

EA: (calcd. for repeating units based on NMR)

calcd.: C: 91.38%; H: 7.67%

found: C: 91.20%; H: 7.65%

DSC: T_g: 95 °C; TGA: T_d: 346 °C

P3

¹H NMR (300 MHz, CD₂Cl₂): δ = 0.71 – 2.47 (112H), 2.72 – 3.29 (4H), 3.87 – 4.15 (20H), 4.38 – 4.59 (1H), 6.63 – 6.73 (1H), 7.06 – 7.44 (16H) ppm.

SEC (DMAc + 0.21% LiCl, PMMA-standard): M_n = 24,900 g/mol; M_w = 32,400 g/mol; Đ = 1.30

EA: (calcd. for repeating units based on NMR)

calcd.: C: 68.64%; H: 8.72%; N: 3.11%

found: C: 68.63%; H: 8.70%; N: 3.14%

DSC: T_g: -5 °C; TGA: T_d: 299 °C

P4

¹H NMR (300 MHz, CD₂Cl₂): δ = 1.24 – 2.36 (3H), 6.37 – 7.34 (5H) ppm.

SEC (DMAc + 0.21% LiCl, PS-standard): M_n = 22,400 g/mol; M_w = 28,700 g/mol; Đ = 1.28

EA: (calcd. for repeating units based on NMR)

calcd.: C: 91.90%; H: 7.71%;

found: C: 92.13%; H: 7.79%;

DSC: T_g: 100 °C; TGA: T_d: 387 °C

P5

¹H NMR (300 MHz, CD₂Cl₂): δ = 0.72 – 2.51 (160H), 2.68 – 3.33 (4H), 3.87 – 4.20 (20H), 4.36 – 4.64 (1H), 6.35 – 7.46 (97H) ppm.

SEC (DMAc + 0.21% LiCl, PMMA-standard): M_n = 17,200 g/mol; M_w = 21,800 g/mol; Đ = 1.27 and (DMAc + 0.21% LiCl, PS-standard): M_n = 16,800 g/mol; M_w = 20,900 g/mol; Đ = 1.25

EA: (calcd. for repeating units based on NMR)

calcd.: C: 79.99%; H: 8.25%; N: 1.62%

found: C: 80.14%; H: 8.16%; N: 1.62%

DSC: T_g : 36 °C; TGA: T_d : 314 °C

P6

^1H NMR (300 MHz, CD_2Cl_2): δ = 0.73 – 2.48 (154H), 2.68 – 3.32 (4H), 3.79 – 4.20 (20H), 4.37 – 4.59 (1H), 6.36 – 7.45 (87H) ppm.

SEC (DMAc + 0.21% LiCl, PMMA-standard): M_n = 15,100 g/mol; M_w = 19,500 g/mol; \bar{D} = 1.29 and (DMAc + 0.21% LiCl, PS-standard): M_n = 14,900 g/mol; M_w = 18,800 g/mol; \bar{D} = 1.26

EA: (calcd. for repeating units based on NMR)

calcd.: C: 79.20%; H: 8.29%; N: 1.72%

found: C: 79.00%; H: 8.37%; N: 1.81%

DSC: T_g : 31 °C; TGA: T_d : 308 °C

P7

^1H NMR (300 MHz, CD_2Cl_2): δ = 0.71 – 2.53 (160H), 2.70 – 3.34 (4H), 3.84 – 4.21 (20H), 4.38 – 4.63 (1H), 6.36 – 7.51 (97H) ppm.

SEC (DMAc + 0.21% LiCl, PMMA-standard): M_n = 43,800 g/mol; M_w = 66,200 g/mol; \bar{D} = 1.51 and (DMAc + 0.21% LiCl, PS-standard): M_n = 41,500 g/mol; M_w = 61,100 g/mol; \bar{D} = 1.47

EA: (calcd. for repeating units based on NMR)

calcd.: C: 79.99%; H: 8.25%; N: 1.62%

found: C: 79.69%; H: 8.26%; N: 1.64%

DSC: T_g : 22 and 94 °C; TGA: T_d : 331 °C

P8

^1H NMR (300 MHz, CD_2Cl_2): δ = 0.72 – 2.52 (154H), 2.69 – 3.32 (4H), 3.75 – 4.22 (20H), 4.38 – 4.65 (1H), 6.35 – 7.51 (87H) ppm.

SEC (DMAc + 0.21% LiCl, PMMA-standard): M_n = 36,100 g/mol; M_w = 54,200 g/mol; \bar{D} = 1.50 and (DMAc + 0.21% LiCl, PS-standard): M_n = 34,600 g/mol; M_w = 50,300 g/mol; \bar{D} = 1.45

EA: (calcd. for repeating units based on NMR)

calcd.: C: 79.20%; H: 8.29%; N: 1.72%

found: C: 79.13%; H: 8.26%; N: 1.80%

DSC: T_g : 5 and 84 °C; TGA: T_d : 321 °C

Density measurement of the soft segment of the block copolymer (P1) with a pycnometer:

$$\rho = \frac{(m_1 - m_0)}{(m_3 - m_0) - (m_2 - m_1)} \times \rho_w$$

m_0 = mass of empty pycnometer; m_1 = mass of pycnometer with copolymer; m_2 = mass of pycnometer with copolymer and filled with water; m_3 = mass of water filled pycnometer; ρ_w = density of water (21°C).

$$\rho_{P1} = \frac{(43.7374 \text{ g} - 43.3621 \text{ g})}{(143.2505 \text{ g} - 43.3621 \text{ g}) - (143.2837 \text{ g} - 43.7374 \text{ g})} \times 0.9980 \frac{\text{g}}{\text{cm}^3}$$

$$\rho_{P1} = 1.095 \frac{\text{g}}{\text{cm}^3}$$

Calculation of the volume-ratio exemplary shown for P5 (Ratio_{NMR} [His]:[BA]:[PS] = 1:10:16):

Mass of the hard block: $M_{\text{hb}} = 1666.40 \text{ g/mol}$ ($16 \times 104.15 \text{ g/mol}$)

Mass of the soft block: $M_{\text{wb}} = 1802.38 \text{ g/mol}$ ($520.68 \text{ g/mol} + 10 \times 128.17 \text{ g/mol}$)

Density of the PS/hard block: $\rho_{\text{hb}} = 1.053 \text{ g/cm}^3$ [S6]

Density of the soft block: $\rho_{\text{wb}} = 1.095 \text{ g/cm}^3$

Volume-ratio [hard/soft] = 1:1.04

References:

- [S1] M. Fernández-García, R. Cuervo-Rodríguez, E. L. Madruga, *J. Polym. Sci., Part B: Polym. Phys.* **1999**, *37*, 2512-2520.
- [S2] R. París, J. L. De la Fuente, *J. Polym. Sci., Part B: Polym. Phys.* **2007**, *45*, 1845-1855.
- [S3] R. B. Beevers, *J. Polym. Sci., Part A: Polym. Chem.* **1964**, *2*, 5257-5265.
- [S4] H. Daimon, H. Okitsu, J. Kumanotani, *Polym. J.* **1975**, *7*, 460-466.
- [S5] W. C. Oliver, G. M. Pharr, *J. Mater. Res.*, **1992**, *7*, 1564–1583.
- [S6] <http://polymerdatabase.com/polymer%20physics/Polymer%20Density.html> (last visited: 03.04.2018).